(2)

NAVAL POSTGRADUATE SCHOOL

Monterey, California

THESIS

OPTIMUM DESIGN OF EXPERIMENTS
IN
COMPOSITE RELIABILITY

by

James W. Coleman

June, 1992

Thesis Advisor: Edward M. Wu

Approved for public release; distribution is unlimited

REPORT DOCUMENTATION PAGE

1a. REPORT SECURITY CLASSIFICATION Unclassified	1b. RESTRICTIVE MARKINGS
2a. SECURITY CLASSIFICATION AUTHORITY	3. DISTRIBUTION/AVAILABILITY OF REPORT Approved for public release; distribution is unlimited.
2b. DECLASSIFICATION/DOWNGRADING SCHEDULE	
4. PERFORMING ORGANIZATION REPORT NUMBER(S)	5. MONITORING ORGANIZATION REPORT NUMBER(S)
6a. NAME OF PERFORMING ORGANIZATION Naval Postgraduate School 6b. OFFICE SYMBOL (*If applicable*) 55	7a. NAME OF MONITORING ORGANIZATION Naval Postgraduate School
6c. ADDRESS (*City, State, and ZIP Code*) Monterey, CA 93943-5000	7b. ADDRESS (*City, State, and ZIP Code*) Monterey, CA 93943-5000
8a. NAME OF FUNDING/SPONSORING ORGANIZATION 8b. OFFICE SYMBOL (*If applicable*)	9. PROCUREMENT INSTRUMENT IDENTIFICATION NUMBER
8c. ADDRESS (*City, State, and ZIP Code*)	10. SOURCE OF FUNDING NUMBERS Program Element No / Project No / Task No / Work Unit Accession Number

11. TITLE (*Include Security Classification*)
Optimum Design of Experiments in Composite Reliability

12. PERSONAL AUTHOR(S) James W. Coleman

13a. TYPE OF REPORT	13b. TIME COVERED	14. DATE OF REPORT (*year, month, day*)	15. PAGE COUNT
Master's Thesis	*From* *To*	1992, June 19	121

16. SUPPLEMENTARY NOTATION
The views expressed in this thesis are those of the author and do not reflect the official policy or position of the Department of Defense or the U.S. Government.

17. COSATI CODES			18. SUBJECT TERMS (*continue on reverse if necessary and identify by block number*)
FIELD	GROUP	SUBGROUP	Composite Reliability, Design of Experiments, Information Theory

19. ABSTRACT (*continue on reverse if necessary and identify by block number*)

Many composite material applications require a high degree of safety and functionality. This demands that reliability be incorporated in composite design. The design prediction of reliability requires a parametric model based on the failure processes in strength and life. The estimation of the model parameters requires large data set usually limited by time and equipment. The objective of this investigation is to provide, via simulation, a statistics based rationale of experiment design. The result enables multiple use of limited equipment through scheduled censoring to optimize information.

20. DISTRIBUTION/AVAILABILITY OF ABSTRACT	21. ABSTRACT SECURITY CLASSIFICATION	
☒ UNCLASSIFIED/UNLIMITED ☐ SAME AS REPORT ☐ DTIC USERS	Unclassified	
22a. NAME OF RESPONSIBLE INDIVIDUAL Edward M. Wu	22b. TELEPHONE (*Include Area code*) (408) 646-3459	22c. OFFICE SYMBOL AA/Wt

DD FORM 1473, 84 MAR — 83 APR edition may be used until exhausted; All other editions are obsolete

Approved for public release; distribution is unlimited.

Optimum Design of Experiments
in Composite Reliability

by

James W. Coleman
Lieutenant, United States Navy
B.S.E.E., Virginia Polytechnic Institute and State University

Submitted in partial fulfillment
of the requirements for the degree of

MASTER OF SCIENCE IN MECHANICAL ENGINEERING

from the

NAVAL POSTGRADUATE SCHOOL
June 1992

Author: _____
James W. Coleman

Approved by: _____
Edward M. Wu, Thesis Advisor

_____
C. N. Calvano, Second Reader

_____
Anthony J. Healey, Chairman
Department of Mechanical Engineering

ABSTRACT

Many composite material applications require a high degree of safety and functionality. This demands that reliability be incorporated in composite design. The design prediction of reliability requires a parametric model based on the failure processes in strength and life. The estimation of the model parameters requires large data set usually limited by time and equipment. The objective of this investigation is to provide, via simulation, a statistics based rationale of experiment design. The result enables multiple use of limited equipment through scheduled censoring to optimize information.

TABLE OF CONTENTS

LIST OF FIGURES

ACKNOWLEDGEMENTS

I would like to express my most sincere appreciation to my wife, Vicky, and daughter, Hannah, for their constant support both in the pursuit of the Master's Degree and the in development of this thesis. The sacrifices they endured were great and will never be forgotten.

Heartfelt thanks go to my Professor Edward M. Wu, my thesis advisor, for caring enough to dedicate many hours and days to my education. He has made this graduate experience everything it was meant to be.

I would also like to express thanks to Associate Professor Charles Calvano for his time and thoughtful recommendations regarding the editing this document.

Finally, I say thank you to the United States Navy for providing me this educational opportunity.

I. INTRODUCTION

The use of fiber reinforced composite materials in load bearing structures has many advantages over conventional materials such as steel and aluminum. The high stiffness to weight ratio, strength to weight ratio, and resistance to corrosion are among the more commonly known advantages. Perhaps the most significant, but not widely known benefit of using composites is the redundancy intrinsic in the material. The redundancy results from the load being shared among a multitude of fibers imbedded in a binding matrix material. However, in order to realize the benefit of increased redundancy, it must be quantified in terms of reliability; i.e. the mathematical model and the parameters specific to the composite require determination.

As with any structural design, it is imperative that reliability considerations be incorporated in the engineering design of a composite. Depending on the application, this may take the form of either functional reliability or human-safe reliability. Functional reliability refers to the level of assurance that the system under consideration will function within the

specified design parameters over the design life. If the life or injury of a human being is at stake, the issue becomes one of human-safe reliability. In either case, a description is required of how the material used in the design will behave under a given stress over time. This description is not possible without empirical data of the material in both strength and life.

Strength and life data for conventional materials can be located in many material and design reference books. The reason for this is that those materials have been in use for so many years that the accumulated data is sufficient to adequately describe the relevant failure processes with a parametric model. This is not the case in the use of the composite materials, for numerous reasons. Composites have a relatively short history of use, and when utilized, the applications are typically considered high technology. High technology applications normally do not produce large numbers of sample sets. Being on the cutting edge means limited lead time, which further complicates the problem of reliability characterization. This limited base of failure data requires that experiments be performed in order to make it possible to understand how the composite behaves in time under load and to estimate the associated parameters of the relevant probability model.

Experiments, however, can be extremely costly in terms of both resources and time. In particular, life experiments present a formidable problem because of the large variability in life data. The large variation in the life data means that a substantial amount of time will pass, possibly hundreds of years, before all samples on test fail. Surely the designer is not going to wait to actually observe even the mean life of such a material in a life test. The solution to this problem, and the objective of this study, is to design the experiment to maximize the amount of information obtained under constrained resources and time. In order to achieve this objective, simulation is required because reliability is probabilistic, involving many combinations of the random variables. The problem, therefore, cannot be directly cast in terms of classical optimization techniques. An objective function cannot be specified to be minimized because the functions and the parameters of the function are not deterministic.

The process simulated in this work is the random nature in which actual materials fail in both load exceedance (strength) and time exceedance (life). The random sets of computer generated failure data are used to simulate the kinds of results an actual experiment might produce. The intended methods of data analysis, such as non-parametric and parametric methods, are then

applied to the simulated data to determine if they will be adequate to produce the desired level of confidence in quantifying the material reliability. In the parametric approach, a model is selected based on the physical failure process of a sample in strength or life. For the known model, the parameters of the model require determination. Since the parameters themselves are probabilistic and will never be known precisely, they can only be estimated. Simulation is used to determine the impact on the statistics of the estimated parameters when a proposed experiment procedure is executed.

The criterion which will be used to evaluate the knowledge gain resulting from one method of performing an experiment compared to another is the change in the information of the parameters. The information of a parameter is quantified through the application of information theory. Information will be shown to be a scalar value, which can be used as an optimality condition in the design of the experiment. In an optimization sense, the design variable is the choice of when to censor an experiment prior to the completion of all the tests to allow the multiple use of limited equipment in order to maximize the objective function of information.

The methods of optimizing information in an experiment developed in this study through the use of simulation are being applied to a graphite fiber

life experiment in progress at the Mechanics of Materials for Composite Reliability Laboratory of the Naval Postgraduate School, Monterey CA.

II. BACKGROUND

The purpose of this chapter is to provide the background information which motivated this investigation. This chapter is divided into three sections: methodologies of design life in engineering, the composite failure mechanism, and information theory. The first section is a contrast of the factor-of-safety and reliability approaches used in engineering design to determine the design life of a component or system. The second section is a description of the failure mechanisms of the composite in strength or life. The final topic is a discussion of information theory and how this concept might be implemented in the design of an experiment.

A. METHODOLOGIES OF DESIGN LIFE IN ENGINEERING

There are two different approaches used in mechanical engineering design to determine the design stresses and/or life of a component or system. They are known as the deterministic or factor-of-safety approach and the reliability approach [Shigley and Mischke,1].

1. The Factor-of-Safety Approach

This approach is based on the assumptions that the applied stresses, strength, and life of a specimen are deterministic. Since a probabilistic model is not needed, this method is simple to use in the design process and is popular for that reason. It is applicable for materials with extended engineering applications where experience can be used to adjust design parameters.

A common method used in the factor-of-safety approach to obtain the design life of a component subjected to alternating and steady stresses is the implementation of the stress versus number of cycles to failure curve (S-N curve). The S-N curve is obtained by placing test samples under specific stress levels and counting the number of stress reversals or cycles up to the sample failure. For materials whose life is sensitive to the duration of stress, a similar curve could be constructed for static stress or for cases where time rather than cycles is the random variable. This is done by having the abscissa represent time to failure rather than cycles to failure.

The S-N curve provided in Figure 2.1 exhibits the features of typical curves obtained for many materials. The term endurance limit (S_e) is used to define the stress at which the slope of the S-N curve is flat or

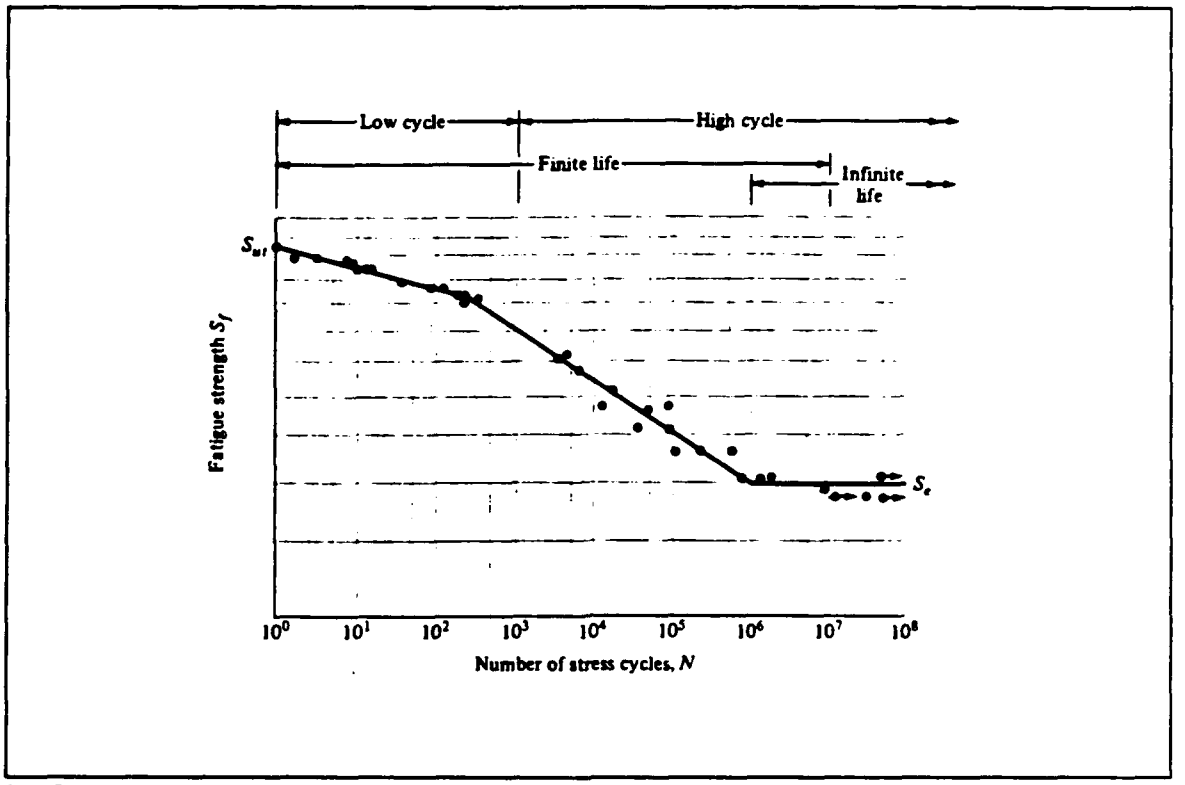

FIGURE 2.1 TYPICAL S-N CURVE [SHIGLEY AND MISCHKE, 1]

approaching zero. This infers that for a design stress with a magnitude less than the endurance limit, the material will have infinite life. Since the material will have infinite life, the design life is no longer required to be a design parameter and is removed from the analysis. However implicitly, additional experience-based modifications are needed to describe the stress time history.

There are fatigue failure methods used in design which are based on the existence of an endurance limit partitioned into the constant stress

time history (mean stress) and the alternating stress time history (cyclic stress). Three of the more common theories are the Soderberg, Modified Goodman, and Gerber criteria. These failure theories can be used to compute a safety factor for stress for particular values of mean and alternating stresses in the design, or to determine the mean or alternating stress corresponding to a desired factor of safety in life.

There are two major shortcomings in using the S-N curve in design. The first shortcoming is that in physical systems, there is no such thing as infinite life. The factually observed failures at a stress lower than the endurance limit cannot be quantitatively defined. In fact, because the slope of the S-N curve is approaching zero, life is not single valued in terms of stress; i.e. according to the S-N curve small variations in applied stress levels will give rise to infinite variability in life.

The second shortcoming is that the incremental increase in safety or functionality which results, for example, when a safety factor of 2 is used instead of 1.75 cannot be quantified. Therefore, the reliability approach is required to rationally answer the question often posed in the design process as to what is the likelihood that a component under design will fail in the service life.

2. Reliability Approach

The reliability approach is based on the formulation that the applied stresses, strength, and life used in design are not deterministic. The objective is to select the random variables salient to the failure process, and describe these variables by either a nonparametric or parametric distribution so that a probable value for the component or system reliability can be calculated. The random variables required to determine the reliability of a composite structure are the applied stress and the duration of time for which the stress is applied. The realizations of the random variables are the stress at failure of the structure (strength) and the duration of time up to failure (life). The failure of a structure, therefore, is represented as a joint probability distribution in strength and life, in lieu of the S-N curve described in the previous section. Pragmatic safety factors are no longer required because the reliability of the component is quantifiable with this joint distribution.

As an illustration of why the determination of the distributions is important, consider schematically the joint probability of failure distribution for a material in Figure 2.2. In this figure, the locii of the median failures is a solid line representing 50% of the samples that would have failed. The

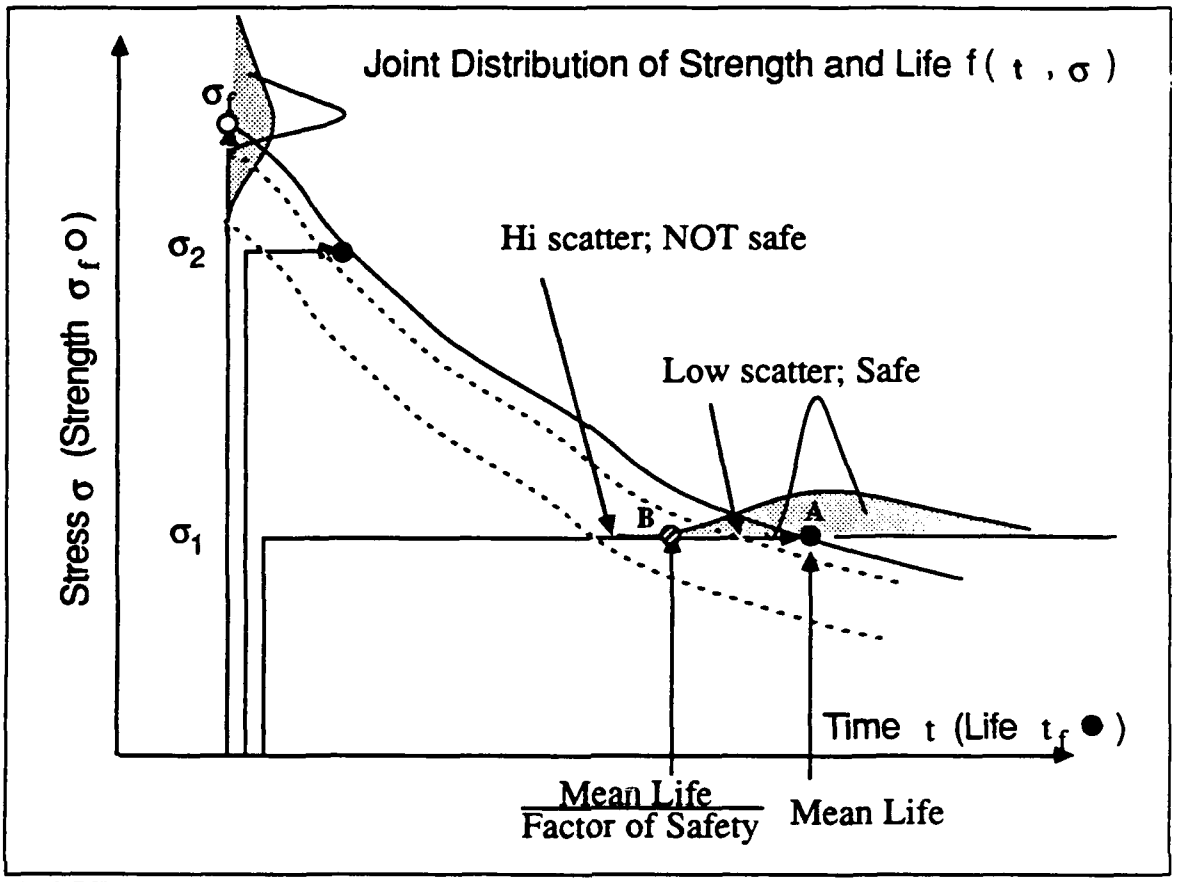

FIGURE 2.2 JOINT PROBABILITY DISTRIBUTION OF STRENGTH AND LIFE

way in which this curve is used is that the designer will enter the graph with the service stress and determine the mean life corresponding to that stress. This point is denoted as point 'A' in Figure 2.2. In the factor-of-safety approach, this mean life will be reduced by some safety factor to the design point labelled 'B' in the figure, which becomes the design point. The dotted line closest to the median curve in Figure 2.2 represents the loci of points for the maximum allowable number of failure, say 0.01%, for the case where the

distributions of the strength and life data have small variability. With respect to the design point, this is a safe design, as the probability of failure is very low for desired stress and service life. The dotted line furthest from the median curve in Figure 2.2 is the loci of the points of the same maximum allowable number of failure (0.01) but for a distribution representing larger variability in the strength and life data. This situation is higher risk with respect to the design point, because although the design appears safe relative to the curve of median failures, the actual probability of failure is larger than the specified maximum.

This clearly shows why the reliability approach results in a much safer design. The S-N curve used in the factor-of-safety approach does not contain any information as to how the failures are distributed about the mean values. This approach is useful only when a large amount of data or experience is available for the materials used in the design where an appropriate safety factor can be pragmatically chosen. In the use of composite materials which utilize high technology fibers such as graphite, the data or experience in the material is not sufficient to warrant the use of safety factors. The relevant data must, therefore, be obtained from

experiments which are designed to produce the greatest knowledge of parameters for describing the distribution of the failure data.

B. COMPOSITE FAILURE MECHANISMS

1. Strength Model

In order to model the failure mechanism of a composite in strength, it is necessary to understand how the fiber and matrix constituents interact when the structure is stressed. A fiber-reinforced composite consists of many long, small diameter fibers embedded in a matrix binder material. The role of the fibers is to act as the load carrying members in the material whereas the matrix serves to transfer the load from broken to adjacent non-broken fibers. If the stress at a point in the structure is high enough to cause a weak fiber to break, the matrix transfers the load from the broken fiber to its surrounding intact neighbors. The majority of load transfer occurs in the immediate vicinity of the break and decreases as the distance from the break is increased. This is shown graphically in Figure 2.3.

Rosen [2] developed a relationship quantifying the distance required for the matrix to transfer the stress resulting from a broken fiber to the surrounding fibers. This quantity is called the ineffective length, and is

given in equation form as follows:

$$\delta = \left\{ \left(V_f^{-\frac{1}{2}} - 1 \right) \frac{E_f}{G_m} \right\}^{\frac{1}{2}} \cosh^{-1} \left\{ \frac{[1+(1+\phi)^2}{2[1-\phi]} \right\} d_f \qquad (2.1)$$

where: V_f is the volume fraction of the fiber
E_f is the modulus of the fiber
G_m is the shear modulus of the matrix
ϕ is the fractional value, called the fiber load sharing efficiency, below which the fiber is not considered effective.

The transfer of stress between neighboring fibers within an ineffective length will occur until the neighboring fibers themselves fail because of the increased stress. As the load is increased, the number of fiber failures will increase, which will eventually lead to the clustering of fiber failure sites. The result is that the local stress concentration is so great that the entire structure catastrophically fails.

Knowledge of how the fiber fails in strength is therefore essential for the description of composite failure. A fiber failure will occur at the statistically weakest segment of the fiber, which may or may not be located at a point of high stress in the structure. Since the failure of the fiber is one

of extreme value governed by the weakest element, the Weibull distribution is used to model the failure process. The cumulative distribution function (CDF) using the Weibull distribution is

$$F(x_i) = 1 - \exp\{(-(\frac{x_i}{\beta})^{\alpha}\} \tag{2.2}$$

The probability of failure of a fiber corresponding to a particular load can be computed using this model once the shape α and location β parameters are known.

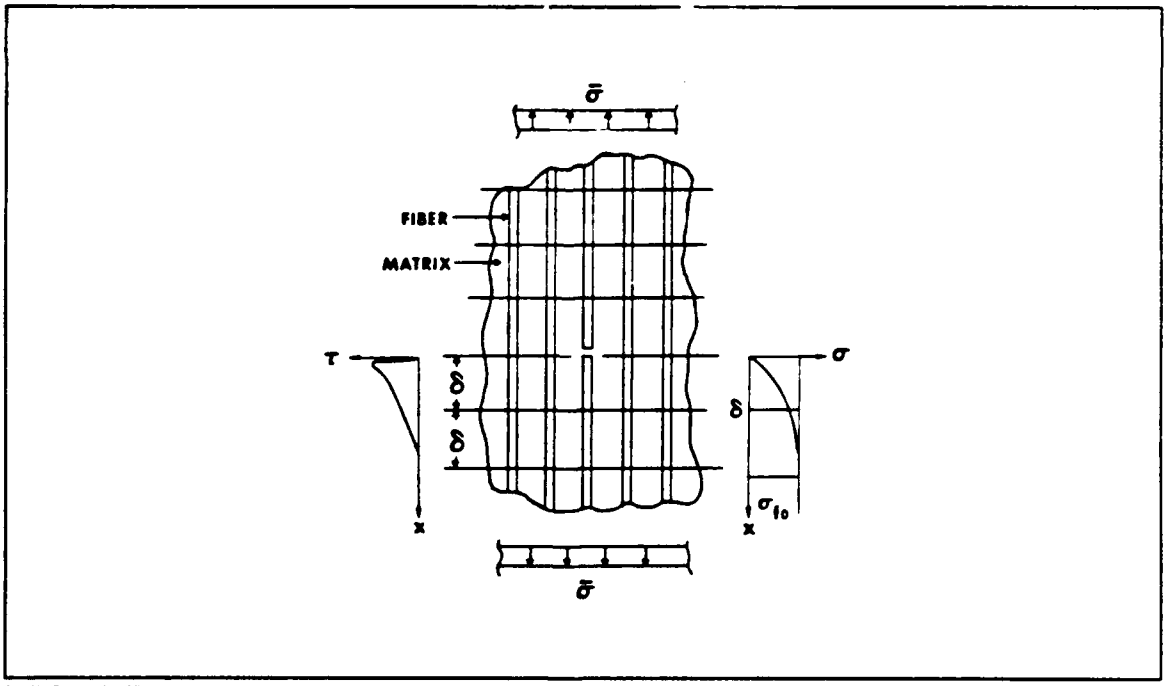

FIGURE 2.3 TENSILE FAILURE MODEL [ROSEN, 2]

In order to determine the strength of the composite, it is necessary to address the combinatorial probability of grouping of fiber failure sites. The model which describes this chanced clustering of fiber breaks was developed by Harlow and Phoenix [3,4] and is known as the Harlow and Phoenix Local Load Sharing model. In this model, a recursive relationship is used to predict the probability of failure based on the fiber strength distribution, all of the possible combinations of adjacent fiber breaks, and the resulting stress concentrations from those breaks within an ineffective length. If the number of adjacent breaks exceeds a critical value k, then the structure will catastrophically fail.

The Harlow-Phoenix Local Load Sharing model was modified by Wu and Harlow to incorporate multi-modality in the fiber strength distributions which occur in the regions of low and high probabilities of failure. These regions will be subsequently referred to as the lower tail and upper tail, respectively. The resulting model is known as the Tri-modal Local Load Sharing model.

2. Strength and Life Model

The time dependence of mechanical breakdown of fibers was pioneered by B. Coleman [5] in 1958. Coleman developed the theory of

breaking kinetics, which is concerned with the problem of calculating the probability that a fiber breaks in a given interval of time when an ensemble of fibers is subjected to a loading history. In this theory, he develops a breakdown function $\Omega(t)$ which is a measure of the breakdown in small subdivisions of the fiber, called slabs, which occurred under a loading history. Coleman concluded that the failure of a fiber ensemble is described by a death potential $\psi(\Omega(t))$; a function of the breakdown function. The interpretation is that the damage ψ of the fiber is measured by the damage history $\Omega(t)$.

Phoenix and Wu [6] provided an overall synthesis of strength and life. The CDF for the time dependent failure of a fiber, in terms of Coleman's damage potential, was shown to have the form

$$F(t;l) = 1 - \exp\{-\psi[\int_0^t \kappa(l(s)ds]\} \ , \ t \geq 0 \qquad (2.3)$$

where: $l(t)$ is the stress history
$\kappa(\cdot)$ is the breakdown rule or damage function
$\psi(\cdot)$ is the shape function (death function).

They were able to cast the damage function in terms of an algebraic form which, when plotted, resembles the strength-life curve shown in Figure 2.2.

Once the time dependent failure properties of the fibers are known, a Local Load Sharing model with time dependent ineffective length and strength may be developed. This is possible because the failure mechanism of the composite in life is analogous to that in strength (i.e., local load sharing among neighboring fibers), with the exception that both the strength of the fiber and the ineffective length δ, which is matrix dominated, may change over time. The life of the composite system is described by a function of either a time dependent fiber strength element or a time dependent ineffective length or both.

There are currently life tests in progress for AS-4 graphite fiber and composite strands of the AS-4 fiber at the Mechanics of Materials for Composite Reliability Laboratory at NPS. The overall objective of the tests is to produce strength-life data in order to determine the parameters of the failure model and define the time dependency of the ineffective length so that a joint probability distribution of the composite can be formed based on the properties of the fiber.

C. INFORMATION THEORY

Shannon [7] developed a mathematical theory which dealt with the statistical nature of the problem of reproducing, either exactly or approximately, a selected message in communication. He introduced a quantity H which is a measure of information, choice, or uncertainty in a process. Shannon called this quantity H entropy as it serves as a measure of disorder; and it is defined by the relationship

$$H = -K \sum_{i=1}^{n} p_i \log p_i \tag{2.4}$$

where: $p_1, p_2, \ldots, p_n$ are the probabilities of occurrence of a set of possible events

K is a positive constant (choice of a unit of measure).

Shannon was primarily concerned with the amount of choice which was involved in the selection of an event or how uncertain one is of the outcome. In this regard, he stated that H would have the property of a monotonically increasing function of n if all p_i are equal. The entropy will increase because, with equally likely events, there is more choice or uncertainty.

Lindley [8] extended Shannon's statistical concept of information to the notion of information in an experiment, rather than in a message. He

suggests the following rule of experimentation: "perform that experiment for which the expected gain in information is the greatest, and continue experimentation until a preassigned amount of information has been attained." Lindley further states that the maximum information will result when the probability distribution of the desired parameter is concentrated on a single value of the parameter, and that the information is reduced when there is any uncertainty in the value of the parameter. He defines information I to be

$$I = \int p(\theta) \log p(\theta) \, d\theta \tag{2.5}$$

Note that the form of this equation for information is similar in form to Shannon's equation of entropy (Eq 2.4) with the exception of a lack of the minus sign. This minus sign was omitted because of the major differences in the goals of a person conducting an experiment and a person concerned with the choices in messages. The communication engineer is more interested in maximizing the choice in messages vice having concentration of the distribution on a single value. Hence, the negative in Shannon's expression of entropy. The objective of performing the experiment, however,

is to reduce the uncertainty or increase the information of the parameters, so the negative sign is not utilized in Eq 2.5.

The interest of this investigation is to maximize the knowledge of the parameters of an experiment for composite reliability characterization, under the constraints of equipment and time. The computation of the information I established in Eq 2.5 will allow a measure to be made of how well the parameters of the model are known and measure the amount of increase in information is achieved by testing more samples. In this context, the information can be used as an optimality condition in experiment design.

III. QUANTIFICATION OF RELIABILITY

As stated in the introduction, the quantification of reliability requires experimental data. The often high cost of experiments mandates that the experimental procedure and method of data analysis be selected to glean the most information. Once the data is obtained, the resulting reliability can be quantified using either a non-parametric or parametric approach. Regardless of the preferred approach, the goal is to determine a range of the random variable which can be utilized within a specified reliability level.

This chapter is dedicated to evaluating the advantages and disadvantages of non-parametric and parametric approaches in the characterization of reliability.

A. NON-PARAMETRIC RELIABILITY CHARACTERIZATION

Non-parametric methods of characterizing reliability are based solely on the data obtained, without the analytical modeling of underlying failure processes. As an example of how data is analyzed using a non-parametric method, consider the graphs in Figure 3.1. The graph in Figure 3.1(a) is the underlying distribution of the simulated data set which is represented non-

parametrically in the form of a histogram. The three sample sizes of N=25, 100, and 1000 are typical of the number of data available for materials which have little experience (i.e., very new material), moderate experience, and extensive experience, respectively. In Figure 3.1(b), the histogram of the small sample size of N=25 samples does not produce a meaningful shape which could be utilized for reliability characterization. Little improvement results when the number of samples is increased to N=100, as shown in Figure 3.1(c). The number of samples must be increased to N=1000 and beyond, as illustrated in Figure 3.1(d), before any meaningful resemblance to the underlying distribution can be made. The observation is that non-parametric methods are useful only when large amounts of data are available; and N>1000 is very large for engineering data.

The advantage of using a non-parametric approach is that only data is needed. The disadvantage in the approach is that it is often not practical or possible in the case of time dependent experiments to obtain the large amount of data needed to make this approach produce meaningful results. As a result, reliability predictions for new engineering applications must almost always be based on a proper model with adequately estimated parameters from limited data.

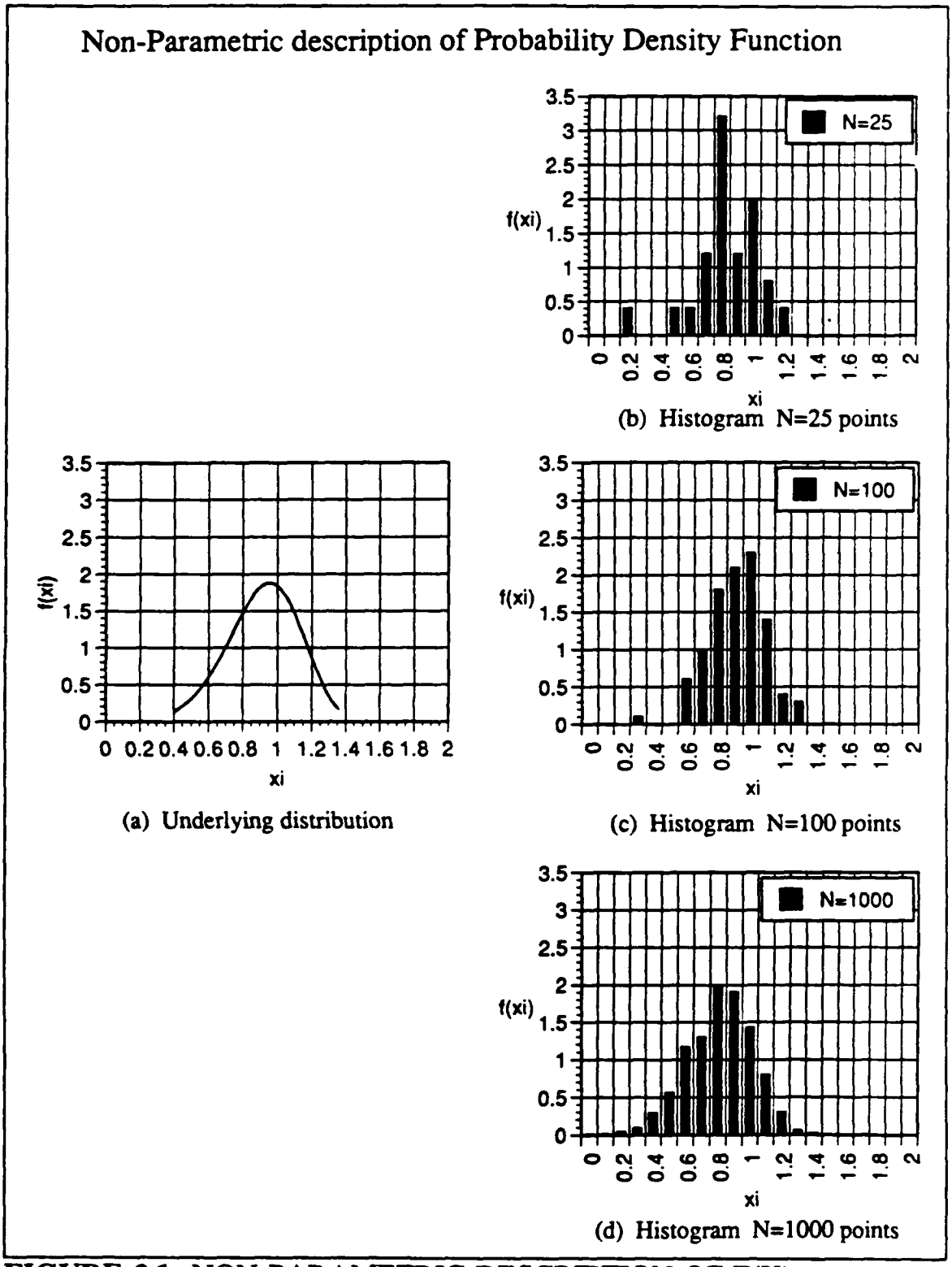

FIGURE 3.1 NON-PARAMETRIC DESCRIPTION OF F(X)

B. PARAMETRIC RELIABILITY CHARACTERIZATION

The prediction of reliability in a parametric sense is based on the selection of an appropriate model and estimation of the associated parameters from data. The model must adequately represent the physical process of the phenomenon being characterized. In the case considered herein, the failure of a graphite fiber in tension is known to be governed by the strength of the weakest segment or link in the fiber. Since it is the presence of a extreme value, such as the weakest link, which causes the failure, the process is modeled using a Weibull distribution. The CDF of the Weibull distribution is given as

$$F(x) = 1 - \exp(-(\frac{x}{\beta})^{\alpha}) \tag{3.1}$$

where: α is the shape parameter
β is the location parameter.

The shape parameter and location parameter α and β are analogous to the reciprocal standard deviation ($1/\sigma$) and mean (μ) used in the Gaussian distribution, respectively. The importance of selecting the correct model cannot be overstated. No matter how diligent the effort is in determining the

parameters of the model, if the model is not correct, the resulting prediction will not be meaningful.

As stated above, the Weibull distribution is known to be the appropriate model for predicting fiber reliability. The problem now becomes one of determining the values of the unknown parameters α and β. Since an infinite number of samples cannot be tested, the true parameters will never be known; they can only be estimated. An estimated parameter, or estimator, will always possess some uncertainty. This introduces the concept that the estimators themselves may be described by a distribution.

The objective in the design of an experiment is to develop a method of conducting the experiment which would result in the estimation of the estimators $\hat{\alpha}$ and $\hat{\beta}$ within a desired range. The circular difficulty in this is that the experimental procedure cannot be planned in advance to produce the desired range of the estimators because little is known about the parameters prior to running the experiment. For example, if the application driving the experiment is one which requires a very high level of reliability, such as a structure in a nuclear safe system, then the estimated parameters will need to be determined with a very small variance from the true values. One may jump to the conclusion that this would require extensive testing and very

large data sets. However, it will be shown in a later section that certain processes have the intrinsic property of small variability in the estimators, so that only a small amount of data would suffice in achieving the certain bounds on the estimators, and the experiment could be planned accordingly. The dilemma is that the existence of this property would not be known without having first conducted the experiment to produce the data. One solution of this dilemma is to use simulation in the design of the experiment. A logical representation of the rationale of incorporating Monte Carlo simulation in the experiment design is provided in Figure 3.2.

The first step of the simulation is to assume the values of underlying parameters for the simulated data set. If possible, the selection of these parameters should be within the anticipated range of values for the underlying parameters of the actual data set so that the simulated process will closely approximate the actual process. Although it is true that little information may be known about the parameters prior to commencement of the experiment, the expected range of parameters can normally be bracketed about a limited range of values. For example, considering the life of a graphite fiber, it is anticipated that the value of the shape parameter of the distribution will be between 0.1 and 1 because of the experience in glass

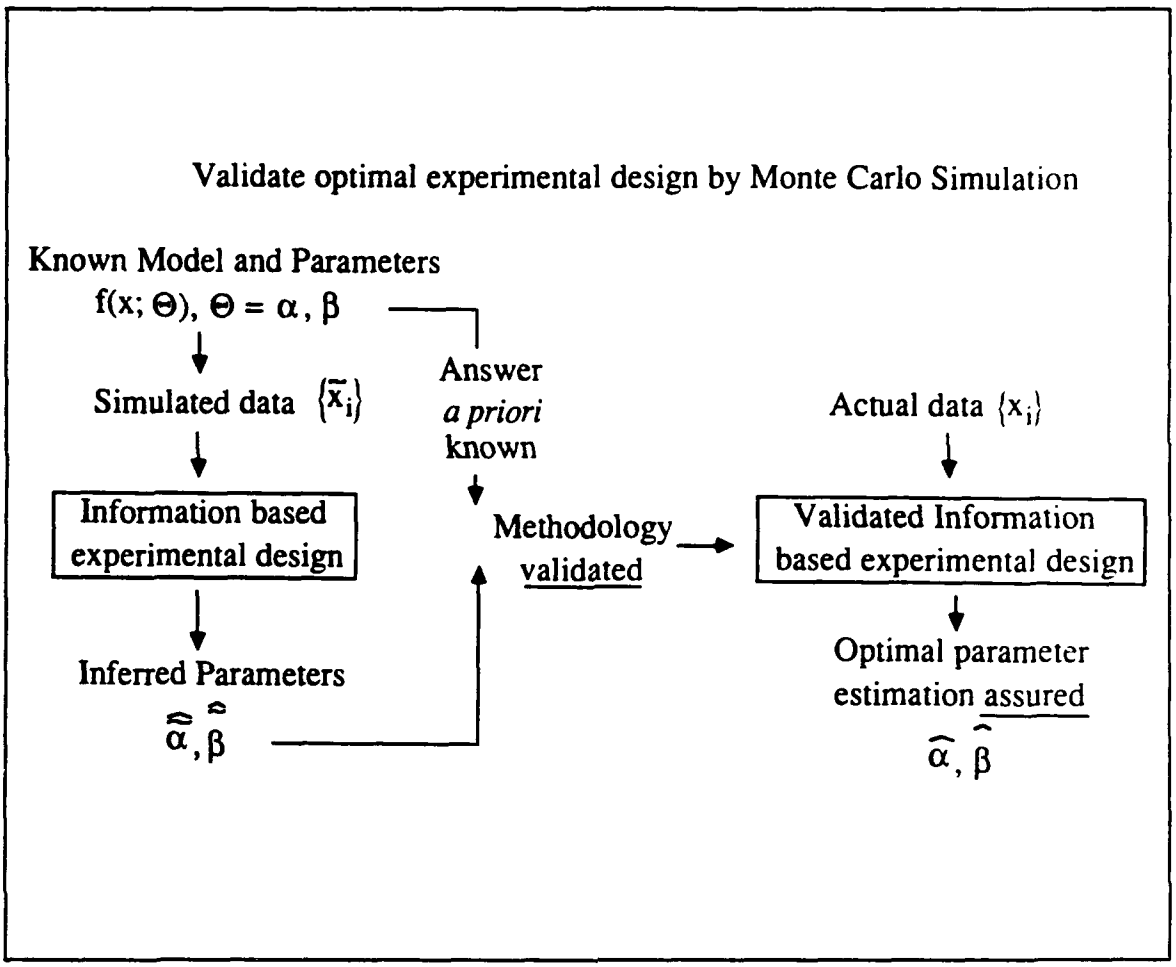

FIGURE 3.2 OPTIMUM EXPERIMENT DESIGN BY MONTE CARLO SIMULATION

fibers and Kevlar fibers. To explore the effects of the experiments, two separate simulations should be run with the underlying values of α assigned in the upper and lower range (i.e., 0.1 and 1) and the proposed procedures can be evaluated accordingly.

The random data set is simulated using the known values of the above range of underlying parameters. Once the simulated data set is obtained, the

experiment design methodology is applied to that simulated set of data. In the case of this study, an information based experimental design methodology is used to obtain optimum estimation of the parameters. The estimated parameters based on the simulated data, denoted $\hat{\hat{\alpha}}$ and $\hat{\hat{\beta}}$, are computed using the prescribed procedure and are compared with the known parameters. If the estimated parameters adequately recover the known values of the underlying parameters, the method is verified and can be implemented on an actual set of data. The analysis of the actual data using the verified information experimental design procedure will assure the optimal parameters estimation.

This section provided an overview of how a random set of data is simulated and how it may be implemented in an experiment design. The remaining portion of this chapter will be dedicated to the presentation of the results of many different simulations conducted and what inferences can be made regarding the role of the parameters in reliability.

C. THE ROLE OF PARAMETERS IN RELIABILITY

In order to determine the role of the parameters in reliability, it is first necessary to distinguish the best graphical domain with sufficient sensitivity

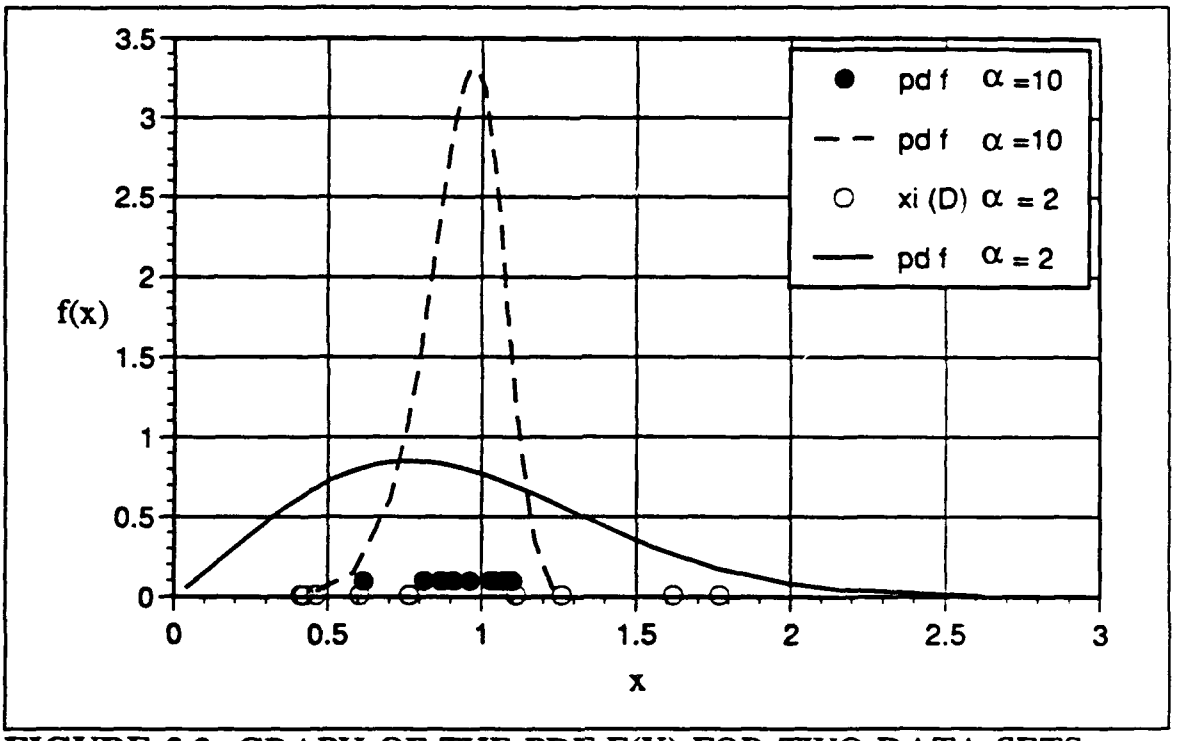

FIGURE 3.3 GRAPH OF THE PDF F(X) FOR TWO DATA SETS

in reliability to identify the uncertainty in one or both of the parameters α and β. The parametric distributions may be presented either as a probability density function (pdf), cumulative distribution function (CDF), or transformed CDF. The transformed CDF, denoted F^*, is a linearized plot of the CDF accomplished by the weakest link transformation of the probability $F(x_i)$ using the relationship

$$F^* = \ln(-\ln(1-F(x_i))) \tag{3.2}$$

and transforming the realized random variable by $\ln(x_i)$. These three plots are shown in Figures 3.3 through 3.5, each containing a plot of distributions

resulting from two simulated data sets of ten each with different values for the parameters as indicated.

Two data sets of ten points each are simulated to illustrate the graphical appearance of data in the three respective probability spaces. One large scatter data set (open circles) and one small scatter data set (solid circles) are simulated from parameters as indicated; the corresponding underlying distributions are respectively shown by solid and dashed lines. In the density space shown in Figure 3.3, the sample number is too small to form a nonparametric empirical pdf, as previously noted in section A of this chapter. Additionally, even if enough data was available for a description of the pdf, subtle changes of the curve in the region of very high levels of reliability, which correspond to low levels of probability of failure (e.g. 10^{-4} and below), are not distinguishable in the pdf domain. This portion of the distribution is called the lower tail, and its shape is the focus of reliability applications. The lower tail is sensitive to variations in the parameters, making it important that this portion of the curve be graphically representable.

While the same small data sets form a more meaningful trend in the CDF space, the lower tail is also obscured. The data points of the simulated data sets are plotted in this domain based on the rank of each sample. The

notion of rank refers to the value of the realized random variable of the sample relative to the sample tested, whereas the true rank is the value relative to all possible samples that exist in the population, tested or otherwise. A further discussion of rank is provided in Appendix A.

The model which best fits this data is provided by the parameters of the model. The estimation of the best fit parameters is performed in the density domain, which results in the likelihood estimators. The likelihood estimators are the most likely parameters based on the observed data. For the Weibull model, the likelihood estimators are denoted $\hat{\alpha}$ and $\hat{\beta}$. Likelihood estimators and maximum likelihood estimators (MLE) are explained in more detail in Appendix B.

Once the estimated parameters are determined using likelihood estimation, the curve representing the CDF may be plotted. The two resulting curves for the two simulated data sets are shown in Figure 3.4. Because the slope of the curves in the CDF domain is approaching zero in the low range of probability of failure they do not provide the resolution to distinguish the lower tail of the curve.

The graph of F^* versus ln (x_i) for the two data sets is provided in Figure 3.5. This graph is useful in reliability because the subtleties in the

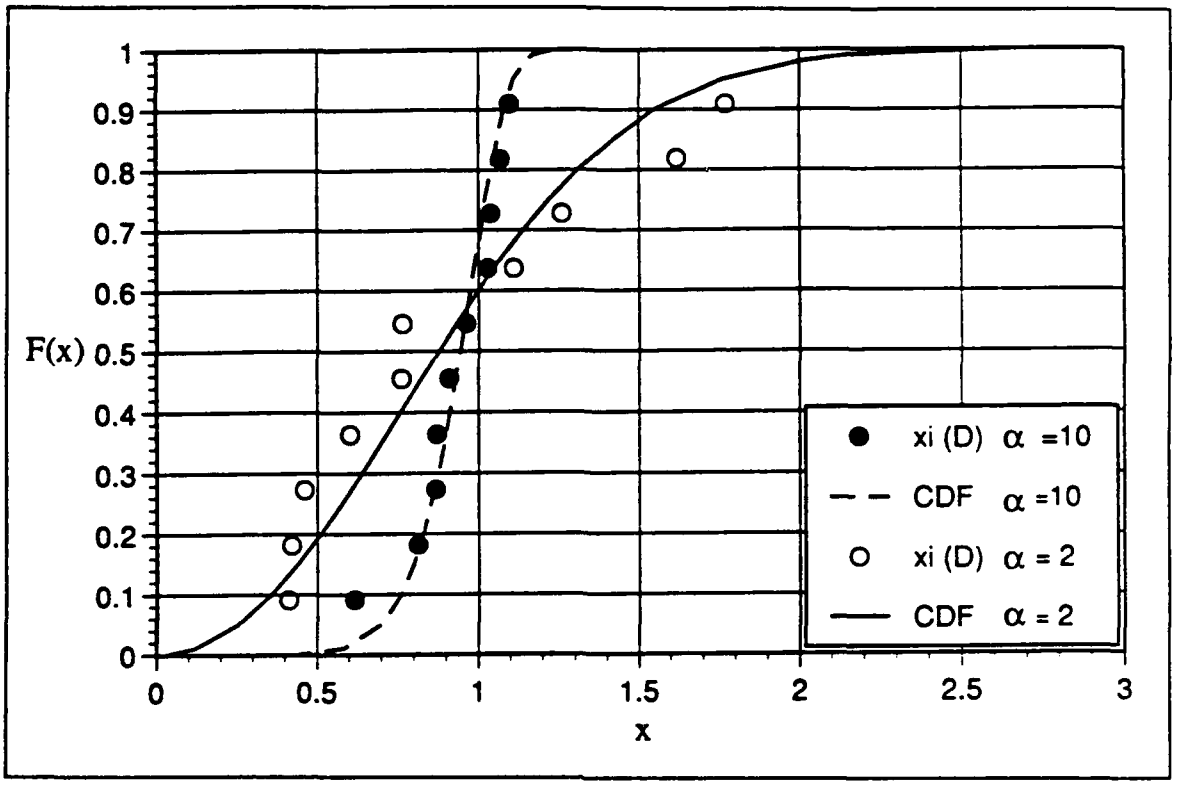

FIGURE 3.4 GRAPH OF THE CDF F(X) FOR TWO SETS OF DATA

lower tail will clearly be evident. There is an additional advantage of using this domain: the shape parameter α is the slope of the line, and the location parameter β is the x value which corresponds to the value of zero on the F^* axis. Wide scattering of data is characterized by a small value of α, or a nearly flat line in the F^* plot; a large value of α corresponds to very little scatter, which is represented by a steep line in F^*.

As previously mentioned, the area of interest in the graph with respect to reliability is the lower left hand portion of the graph which corresponds to the region of low probabilities of failure. This region is referred to as the

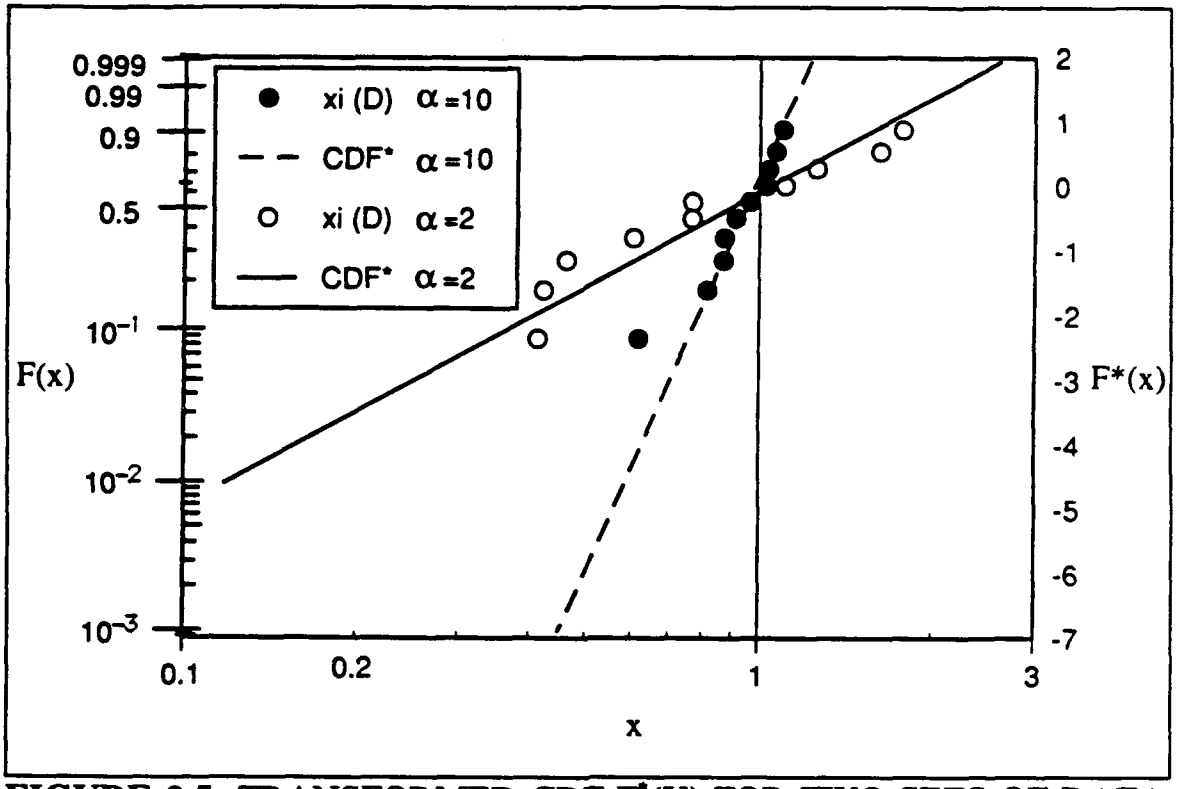

FIGURE 3.5 TRANSFORMED CDF $F^*(X)$ FOR TWO SETS OF DATA

reliability region and is shown in Figure 3.6 as the shaded region in the F^* graph. The top of this region is bounded on the F^* axis by the maximum probability of failure permitted by the design specification, and bounded on the x_i axis by the maximum permitted value of the design variable, also defined in the design specification. For example, the design specification of a composite pressure vessel may state that the vessel should be designed to accommodate a maximum stress of 30 ksi with a reliability of 0.9999. This specification would define a reliability region of 0.0001 on the F^* axis or

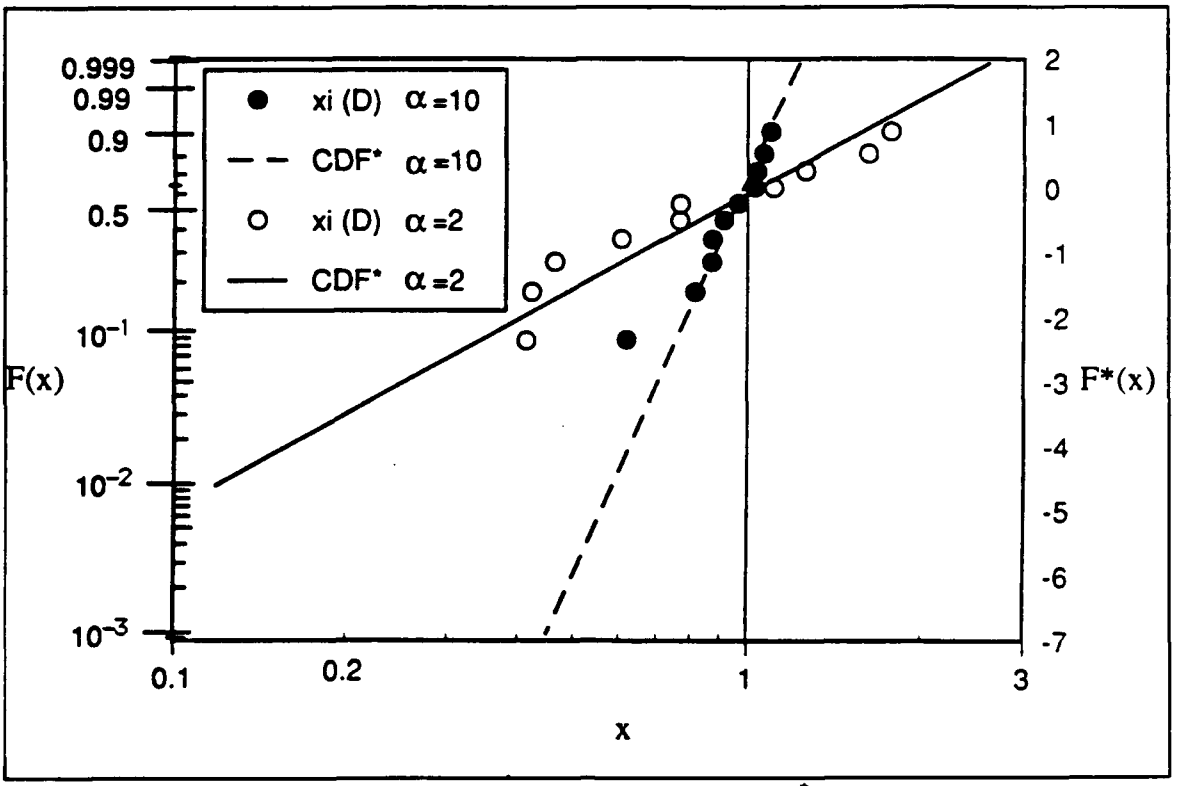

FIGURE 3.6 RELIABILITY REGION IN THE F* DOMAIN

$F \leq (1-0.9999)$ and $x \leq 30$ ksi on the x-axis. A sample of how the reliability region would appear as the shaded region in Figure 3.6.

The reliability region is used to determine whether the object under test will be capable of meeting the design specifications. As an illustration, consider the two linearized curves of the simulated data sets in Figure 3.6. The curve which characterizes the data set with a small amount of scatter (α=10) passes below the reliability region. This is representative of a very safe design, or possibly an overdesign, because the maximum allowed probability of failure is not reached until relatively high values of the random

variable reached. Or stated differently, for the maximum permitted value of the random variable for the design, such as stress for a structure, the probability of failure is much lower than required. The designer may then evaluate whether the cost of this extra safety is justifiable.

The curve representing the simulated data set with a large amount of scatter (α=2) passes above a portion of the reliability region. In this case the design does not meet the required reliability and safety specification for certain values of the random variable. This result would indicate that either the design be reworked to meet the specifications or the specifications be relaxed to accommodate less reliability and safety.

The parameters of the model selected to describe the physical process have been shown to be essential in the quantification of reliability. The reliability region was identified in evaluating the impact of the values for the parameters on the design. The next section will address how the estimated parameters of the model vary with the number of data tested and the type of data obtained from an experiment.

D. STATISTICS OF THE ESTIMATED PARAMETERS

In order to show how the statistics of the estimated parameters vary, multiple simulations were conducted with different numbers of samples in a data set and different values of the underlying parameters. For each simulation run, the MLE parameters were computed for the generated data and tabulated. Since there are two parameters estimated, the relative frequency of occurrence of an $\hat{\alpha}$, $\hat{\beta}$ pair is represented as a three-dimensional histogram. Each column in the histogram would represent the number of occurrences that the MLE parameter fall within a specified band, called the class interval.

The underlying values of the shape parameter α selected for the three simulations are 0.8, 5, and 20. The rationale for selecting these values is that they are numbers which are typical in describing life data for a Kevlar fiber, strength data for a graphite fiber, and strength data for a composite strand, respectively. These numbers not only illustrate the statistics of the parameters in the area of composite reliability, the interpretations can also be extended to data sets in general which are characterized by a large amount of data scatter (α=0.8), intermediate amount of scatter (α=5), and small scatter (α=20). The two sample sizes selected for the simulation are

N=10 and N=100 samples. The rationale for the selection of these two numbers of samples is that they are typical bounds used in the quanification of reliability in engineering design.

The MLE parameters were calculated for each simulated data set of N=10 and N=100 samples and stored. The process was then repeated 10,000 times; resulting in 10,000 $\hat{\alpha}$ and $\hat{\beta}$. The objective of the simulation was to observe any differences which might exist in the distributions of the estimators as a function of the values of the shape parameters and sample sizes.

The location parameter β was not varied in the simulation because the variability can be observed in the normalized form.

1. Inferences on the Statistics of the Parameters based on Simulation

The results of the simulations are provided in Figures 3.6, 3.7, and 3.8. Each figure is a histogram representing the relative frequencies of the estimators and the corresponding marginal distributions which are obtained by projecting the histogram on the $\hat{\alpha}$, and $\hat{\beta}$ axes. Stated mathematically for

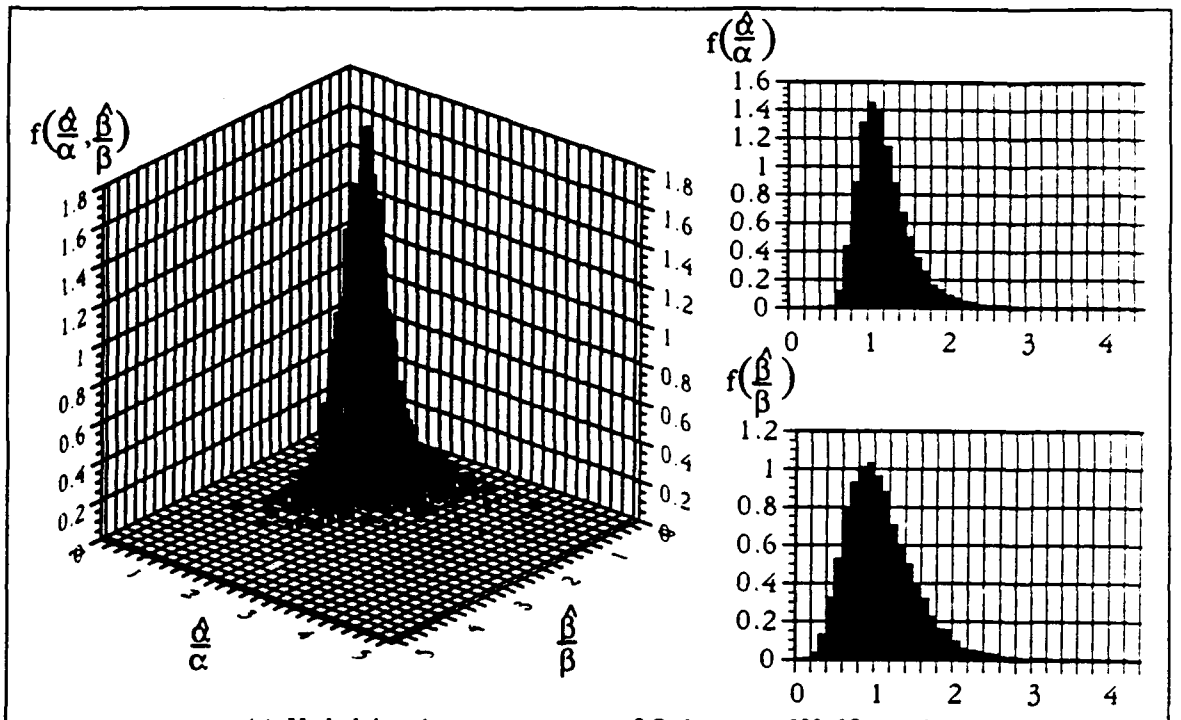

(a) Underlying shape parameter $\alpha = 0.8$, data sets of N=10 samples

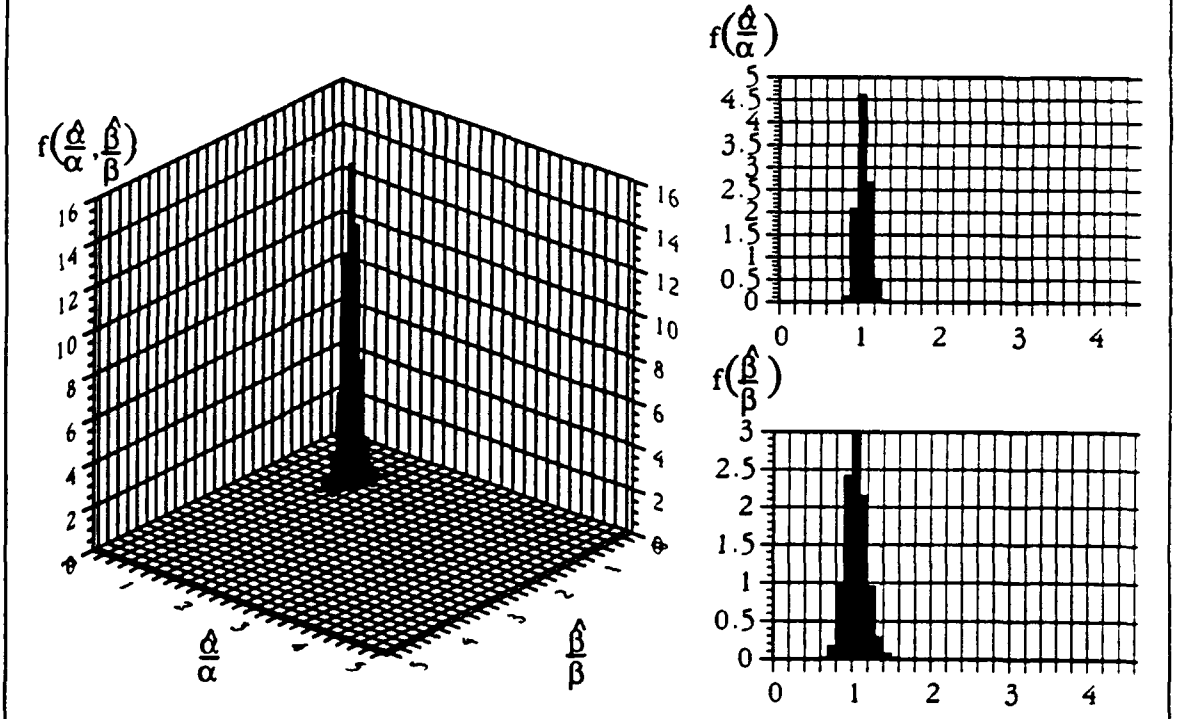

(b) Underlying shape parameter $\alpha = 0.8$, data sets of N=100 samples

FIGURE 3.6 JOINT HISTOGRAM AND MARGINAL DISTRIBUTIONS OF THE ESTIMATED PARAMETERS FOR α=0.8

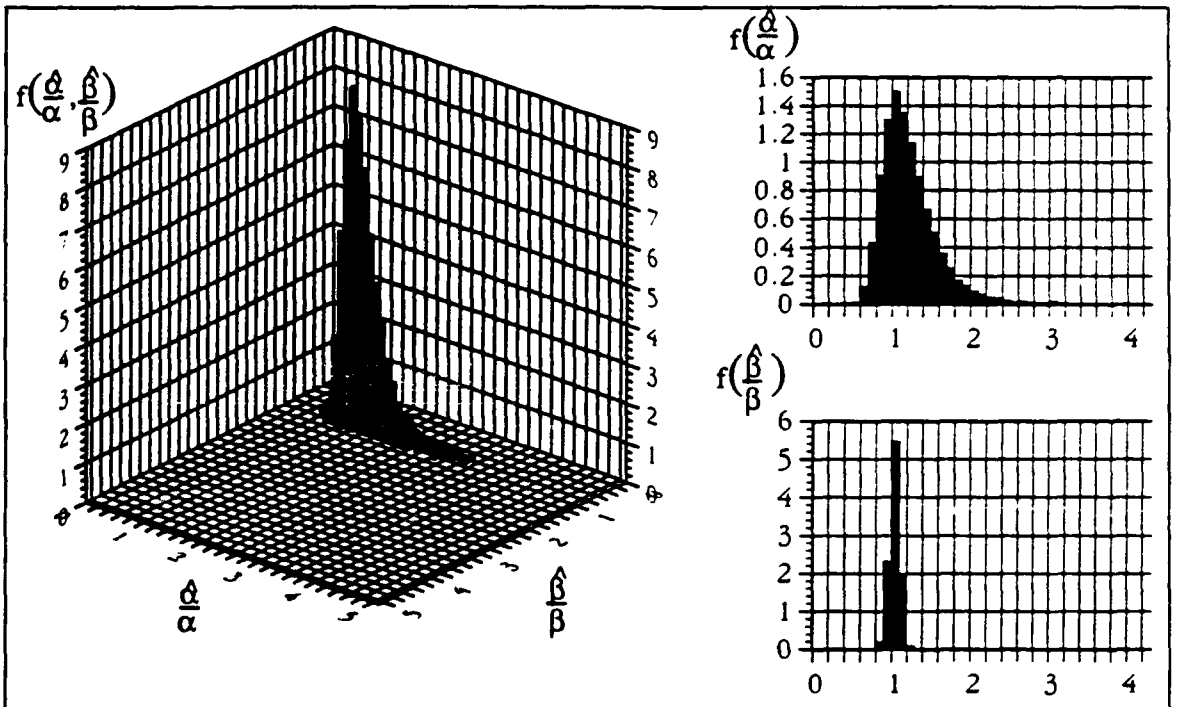

(a) Underlying shape parameter $\alpha = 5$, data sets of N=10 samples

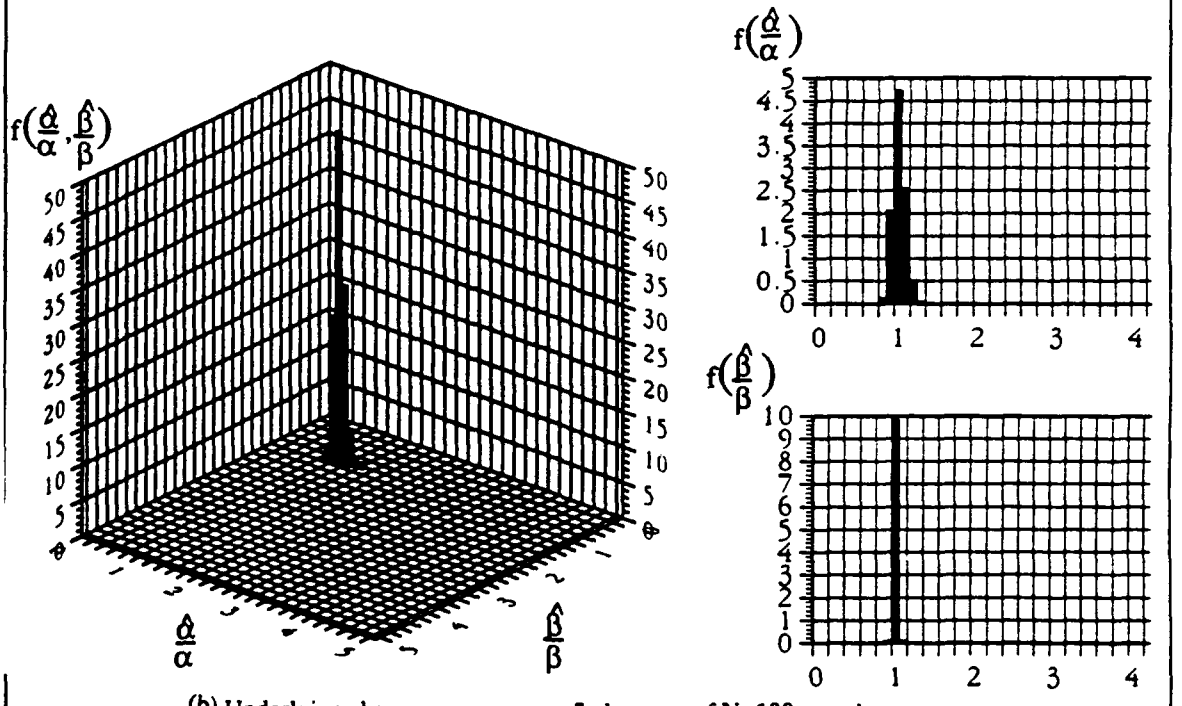

(b) Underlying shape parameter $\alpha = 5$, data sets of N=100 samples

FIGURE 3.7 JOINT HISTOGRAM AND MARGINAL DISTRIBUTIONS OF THE ESTIMATED PARAMETERS FOR α=5

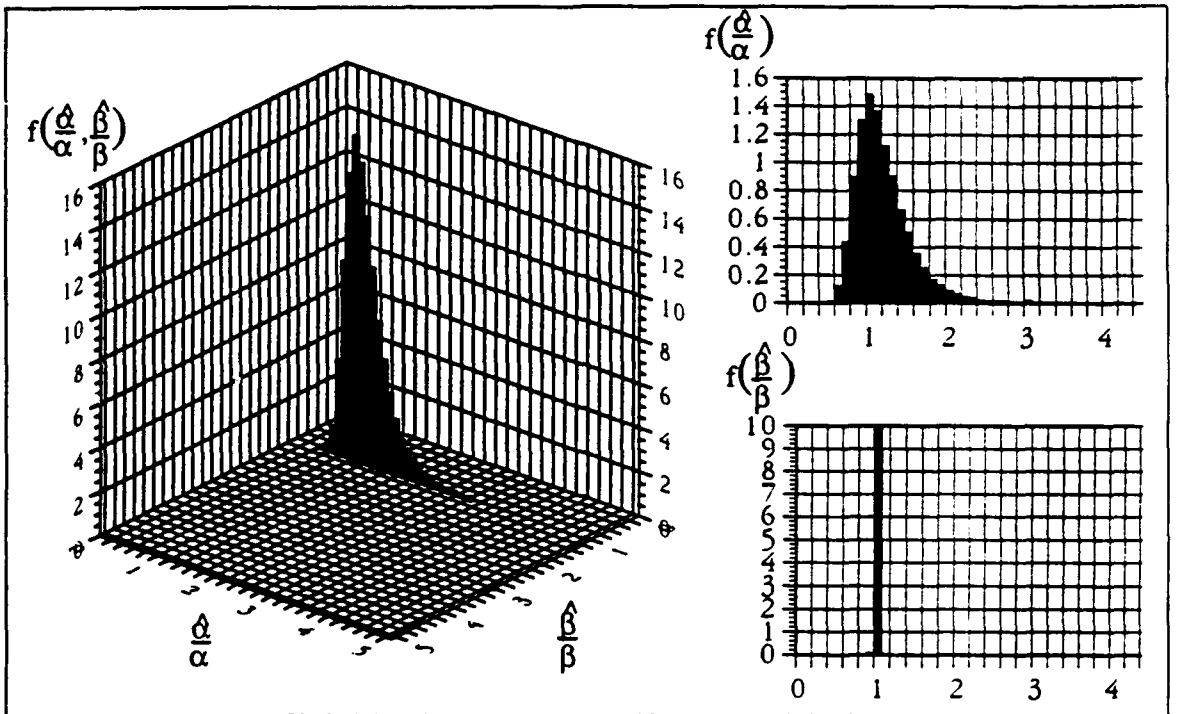

(a) Underlying shape parameter $\alpha = 20$, data sets of N=10 samples

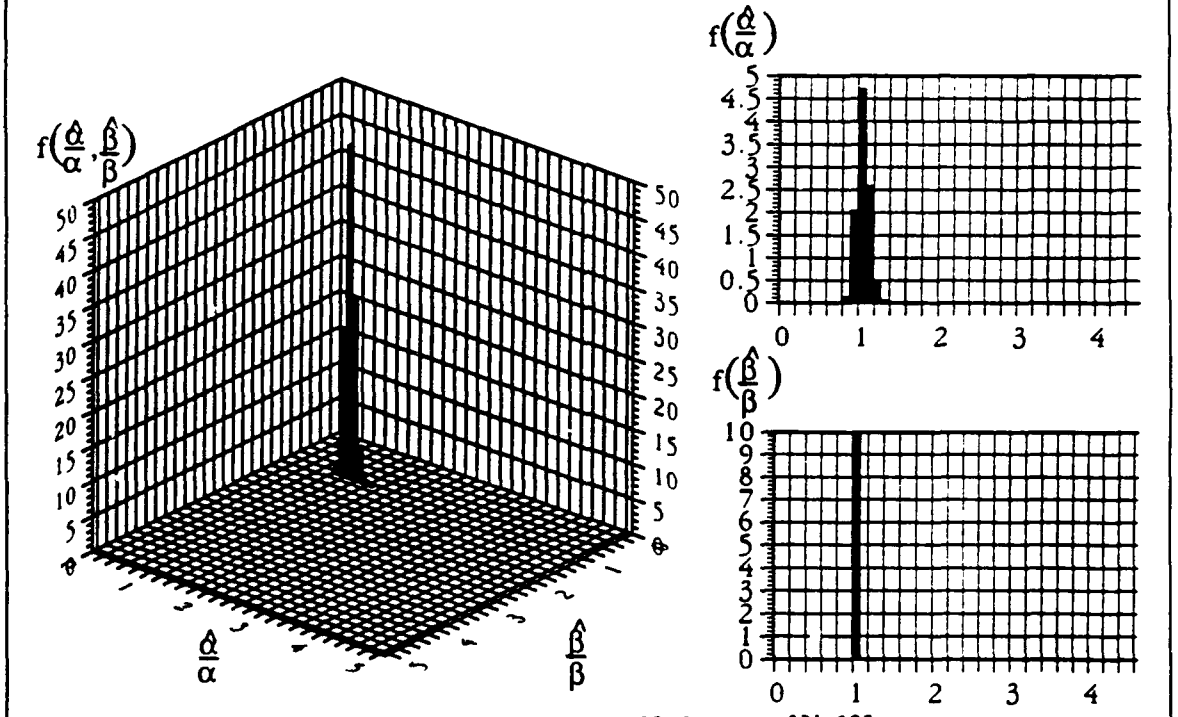

(b) Underlying shape parameter $\alpha = 20$, data sets of N=100 samples

FIGURE 3.8 JOINT HISTOGRAM AND MARGINAL DISTRIBUTIONS OF THE ESTIMATED PARAMETERS FOR α=20

discrete random variables, the marginal distribution is defined as

$$f_x(x) = \sum_n f(x,y_n)$$
$$f_y(y) = \sum_n f(x_n,y) \qquad (3.7)$$

where: $f_x(x)$ are the marginal distributions of the x random variable.
$f_y(x)$ are the marginal distributions of the y random variable.
$f(x_n,y)$ is the joint probability distribution of x_n with y constant.
$f(x,y_n)$ is the joint probability distribution of y_n with x constant.

It is important to note that in each of the histogram or marginal distribution plots, the $\hat{\alpha}$ and $\hat{\beta}$ axes have been normalized by the known underlying values so that the true values will be represented as the number 1.0 on each of the axes.

The histograms and marginal distributions for the case where α=0.8 and N=10 and N=100 are provided in Figure 3.6. The joint histogram in Figure 3.6(a) is characterized by a large scatter of the computed MLE parameter for the case of N=10. This is also evident in the marginal distributions of $\hat{\alpha}$ and $\hat{\beta}$. The scatter was reduced when more samples were tested in each data set, as shown in the case when N=100. In Figure 3.6(b) the marginal distributions of $\hat{\alpha}$ and $\hat{\beta}$ indicate that a tenfold increase in the amount of data in each sample set significantly reduces the uncertainty of

recovering the correct parameters. It is important to note that for both cases where N=10 and N=100, the distribution of the estimated location parameter $\hat{\beta}$ is wider than the shape parameter $\hat{\alpha}$. The overall interpretation is that when α is small (i.e., the data is largely scattered) there exists a large range of parameters which would be likely to describe the data.

The underlying value of the shape parameter α in Figure 3.7 was increased to α=5 in order to represent sets of data that possess an intermediate amount of scatter. For the case of very small sample size N=10, as shown in Figure 3.7(a), the uncertainty in the MLE $\hat{\alpha}$ is approximately the same as that shown for α=0.8. The uncertainty in the location MLE $\hat{\beta}$, however, is dramatically reduced when compared to the $\hat{\beta}$ curve in Figure 3.6(a). The uncertainty in the both estimators is reduced by increasing the sample size to N=100. But as illustrated in Figure 3.7(b), the amount of the reduction in the uncertainty of $\hat{\beta}$ obtained by increasing the number of samples simulated in each data set is not as great compared to the reductions obtained for α=0.8. The interpretations of these results are that since the scatter in the data of the simulated data sets was reduced, the location parameter can be estimated fairly accurately, even with a small

amount of data. The increase in the samples comprising each data set significantly reduced the uncertainty of the estimator $\hat{\alpha}$.

A data set which has little scatter in the data is representable by a large value of the shape parameter. The results of the simulation for this type of data set are provided in Figure 3.8, where α=20. Again, as shown in Figure 3.8(a), the uncertainty in $\hat{\alpha}$ is approximately the same as that obtained for α=0.8 and α=5. Note that the $\hat{\beta}$ is known very well, and the improvement in the uncertainty of this estimator is not detectable when the sample data set is increased to N=100 samples, as illustrated in Figure 3.8(b).

If the goal of the experiment was to estimate $\hat{\beta}$ (the estimator of the location parameter β), then for data which is described by very little scatter (large shape parameter), increasing the number of samples provides little improvement on the level of uncertainty in $\hat{\beta}$. A similar trend is expected for the estimated shape parameter $\hat{\alpha}$. Although this trend was not demonstrated for the series of simulations performed here, it is anticipated that for very high values of α, say α>50, only a small amount of data would be required to estimate the parameter with a high degree of certainty. In the limiting case where $\alpha=\infty$, the curve of the distribution would be a

vertical line in the F^* domain, and only one realization of the random variable would be required to define the parameters.

The influence of the number of samples in the data set and the associated scatter possessed by that data set significantly affects the uncertainty of the estimator. In some experiments, only limited amount of data would be required to determine the parameters; in others generous amounts of data would be needed. It is clear that some form of optimality condition should be devised which would assign a value to the amount of uncertainty in the estimated parameters. The experiment could therefore be designed so that the uncertainty is minimized under the constraints of limited equipment and time. The formulation of this optimality condition is the subject of Chapter IV.

IV. OPTIMIZATION OF INFORMATION IN AN EXPERIMENT

The statistics of the estimated parameters are influenced by both the amount of data obtained from an experiment and the intrinsic scatter in the data. In many cases, large amounts of data are required to estimate the parameters within the desired degree of certainty. However, an experiment will only produce a limited amount of data. Experiments are commonly limited in the time available to conduct them, or by the capacity of the test equipment. In time-limited experiments, such as in life and fatigue tests, production deadlines often limit the amount of time allowed to perform the required testing and resources limit the number of experiments which can be run concurrently. Capacity limited data refers to the situation where the capacity of the test equipment is not sufficient to cause a realization of the random variable. For example, consider the problem of determining the ultimate torsional strength of a propulsion shaft for an aircraft carrier. If the test equipment available does not have the capacity to achieve the predicted failure torque, then the experiment is said to be limited in capacity.

A. CENSORING OF AN EXPERIMENT

Censoring the experiment means the experiment is terminated at either a scheduled value of the random variable or by the number of realizations which have occurred. In a life experiment, scheduled censoring means that the experiment is terminated after a preassigned period of time has elapsed, regardless of the number of samples that have failed. If the life experiment was censored by the number of realizations, then the experiment would be terminated after the predetermined number of samples have failed, regardless of the time it takes for those samples to fail. A capacity limited experiment is essentially a schedule censored experiment because the it will be terminated when a specific value of the random variable is reached, no matter how many samples have failed. Consider the previous example of the aircraft carrier propulsion shaft. If the test equipment in use does not have the capacity to achieve the desired value of torque, then the experiment is effectively censored (scheduled) at the maximum torque that may be achieved by the test equipment.

The question which arises in censoring an experiment is when should the censor be implemented. Is it better, for example, to allow 10 objects on test to proceed for the duration of a three year life experiment, or censor the

experiment at the end of each year and immediately put 10 new samples on test, thereby testing a total of 30 samples for one year each? Further complicating the issue, one may ask whether it might even be more useful to censor every six months, so that the number of repeated tests is six vice three or one. The advantage of censoring every six months is that a total of 60 samples would be put on test as compared 30 samples for the yearly censor, or only 10 samples for the case if no censoring was utilized. The disadvantage of the six month censor plan is that the six months might not be enough time to produce any failures.

A similar decision is required for capacity limited experiments. The censor torque for the aircraft carrier shaft example might be the maximum torque of the test equipment. However, if no shafts fail at that torque because it is low relative to the mean failure torque, then no data is obtained for estimating the parameters of the failure model. What is desired is to know the minimum down-sizing of the shaft for testing so that some failure will be observed, producing useful data for analysis. The reason the largest shaft is desired is to minimize size effect extrapolation from the reduced size test sample size back to actual prototype dimensions.

1. Effect of Censoring on the Estimated Parameters

The solution of when to censor either a time or capacity limited experiment is secured through information of the likelihood function. The reason the likelihood function is chosen for this purpose is that it captures the probability that a specific pair of parameters are the ones which provide the best fit of the data. Since the goal of performing the experiments is to determine the parameters of the failure model, the likelihood function will serve to gauge the effect of early censoring on the estimated parameters.

The likelihood function of Eq B.1 must be revised to account for the samples which did not fail at the point when the experiment was censored. All of the samples which would have remained on test are therefore reliable up to the point of censor. The likelihood function becomes the product of the probabilities of the realized data times the reliabilities of the samples which survived. In equation form, the likelihood function for n exact and c censored samples of N total samples becomes

$$L = \left[\prod_{i=1}^{n} f(x_i)\right]\left[1 - F(x_i)\right]^{N-c} \tag{4.1}$$

Figures 4.1 through 4.3 demonstrate the impact of censoring on the likelihood surface and the corresponding marginal distributions of the shape

parameter α based on the point a simulated experiment is censored. In the simulation, three different numbers of realized data were used as the censor points. Additionally, the simulation was executed for three different values of the underlying values of α. The motivation behind selecting three different censor locations and underlying shape parameters was to evaluate the effect of the number of realized data, denoted n, and the amount of scatter possessed by the experimental data have on the estimated parameters. Two of the values selected for α in the simulations were 0.2 and 1, as they represent typical high and low values for the shape parameter in fiber life experiments. The other value was chosen to be α=5, a commonly observed value for describing fiber strength data. Choosing practical numbers such as these will provide some insight as to how the actual data obtained from the fiber experiments will affect the estimated parameters.

The likelihood surfaces in Figures 4.1(a)-(c) are the result of censoring a simulated experiment of 100 samples which have the intrinsic property of producing a large amount of scatter in the realized data (α=0.2). Each surface has the appearance of a long tunnel parallel to the β axis (the location parameter). The interpretation is that when α is small (large scatter), a large range of β's could equally likely be the underlying location

parameter. The marginal distributions of α, provided in Figure 4.1(d), are obtained by numerically integrating out the β from the likelihood surface. There is minor difference in the shapes of the curves represented by censoring after 5, 10, and 25 realizations. This is an important result because it shows that little improvement in the uncertainty of the estimated parameter is obtained by prolonging the experiment so that 25 failures would occur instead of censoring it after only five failures. This suggests that early censoring is effective for processes described by small values of α. The early censor would therefore effectively allow a larger number of samples N to be tested, resulting in more early failures n to be used in the analysis. The disadvantage of implementing an early censor strategy is that knowledge of the location parameter is sacrificed, because data near the mean value is never realized because the experiment was terminated early. In life experiments, however, for low values of α the mean life is of secondary interest. Recall, the most useful quantity is the shape parameter of the lower tail in the reliability region. The more data which is realized in the area of interest, the better the estimate of the shape parameter.

The effect of censoring a simulated experiment producing a data set described by an underlying α=1 is given in Figure 4.2. The resulting

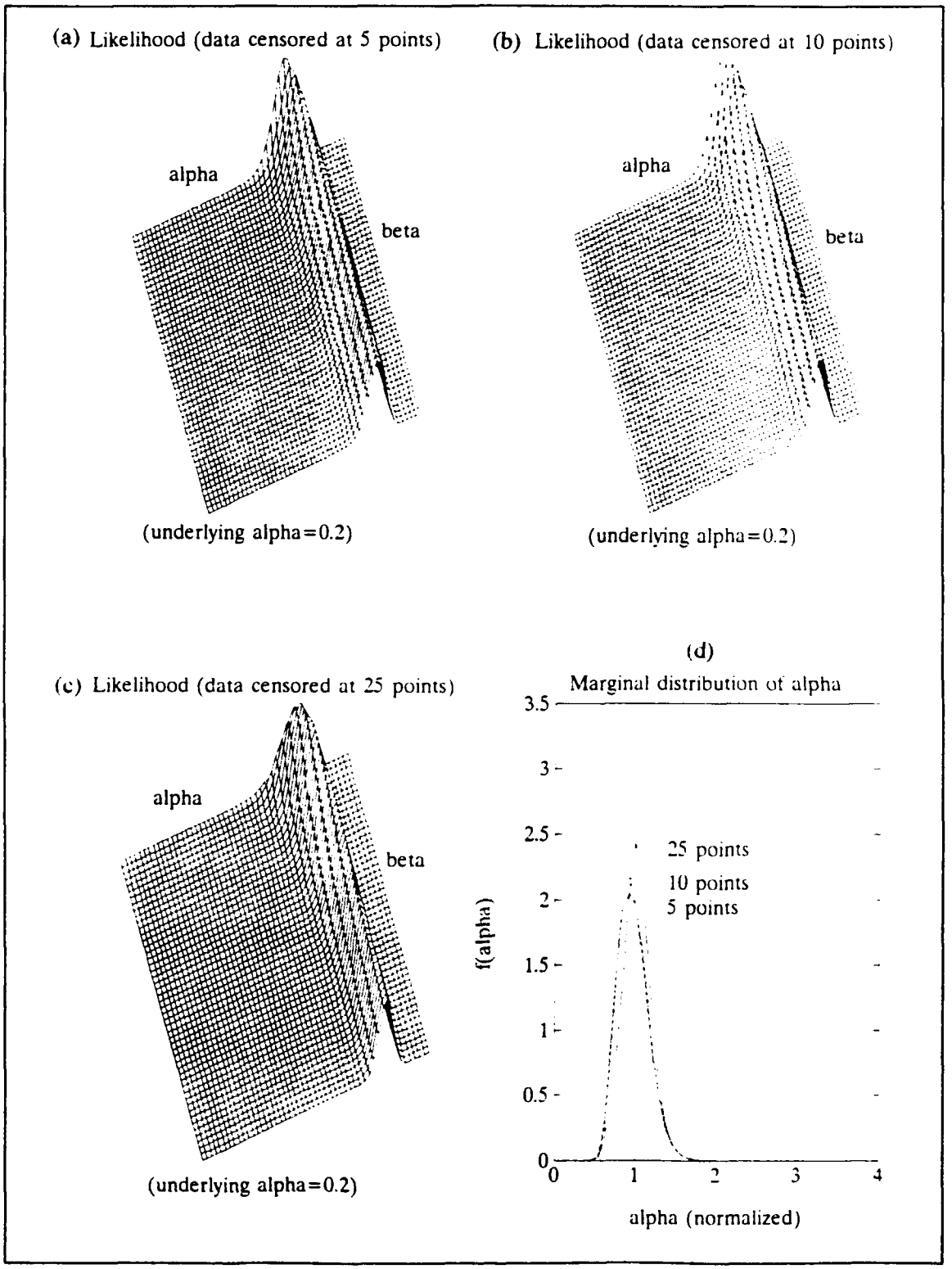

FIGURE 4.1 EFFECT OF CENSORING ON LIKELIHOOD FOR α=0.2

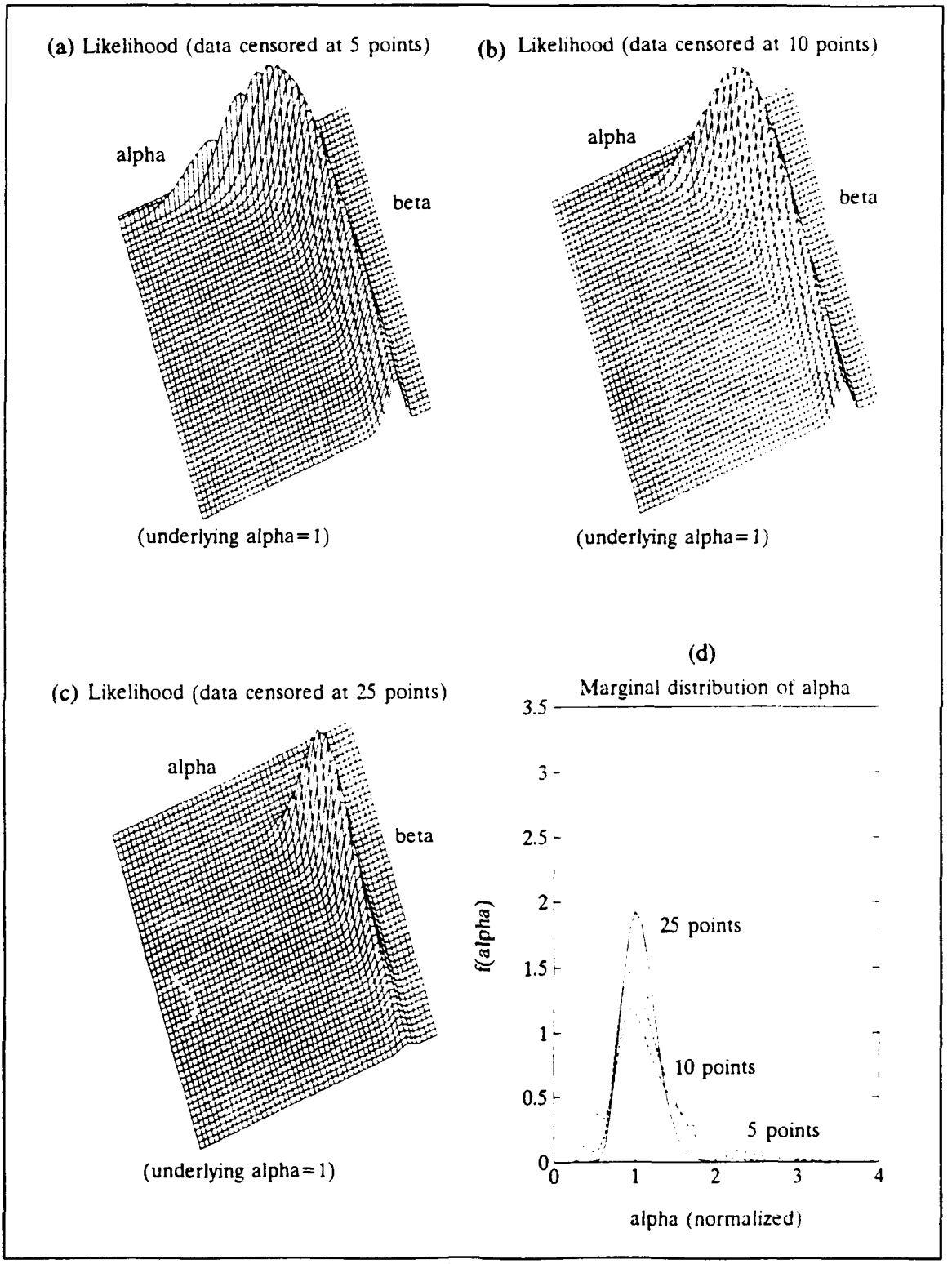

FIGURE 4.2 EFFECT OF CENSORING ON LIKELIHOOD FOR α=1

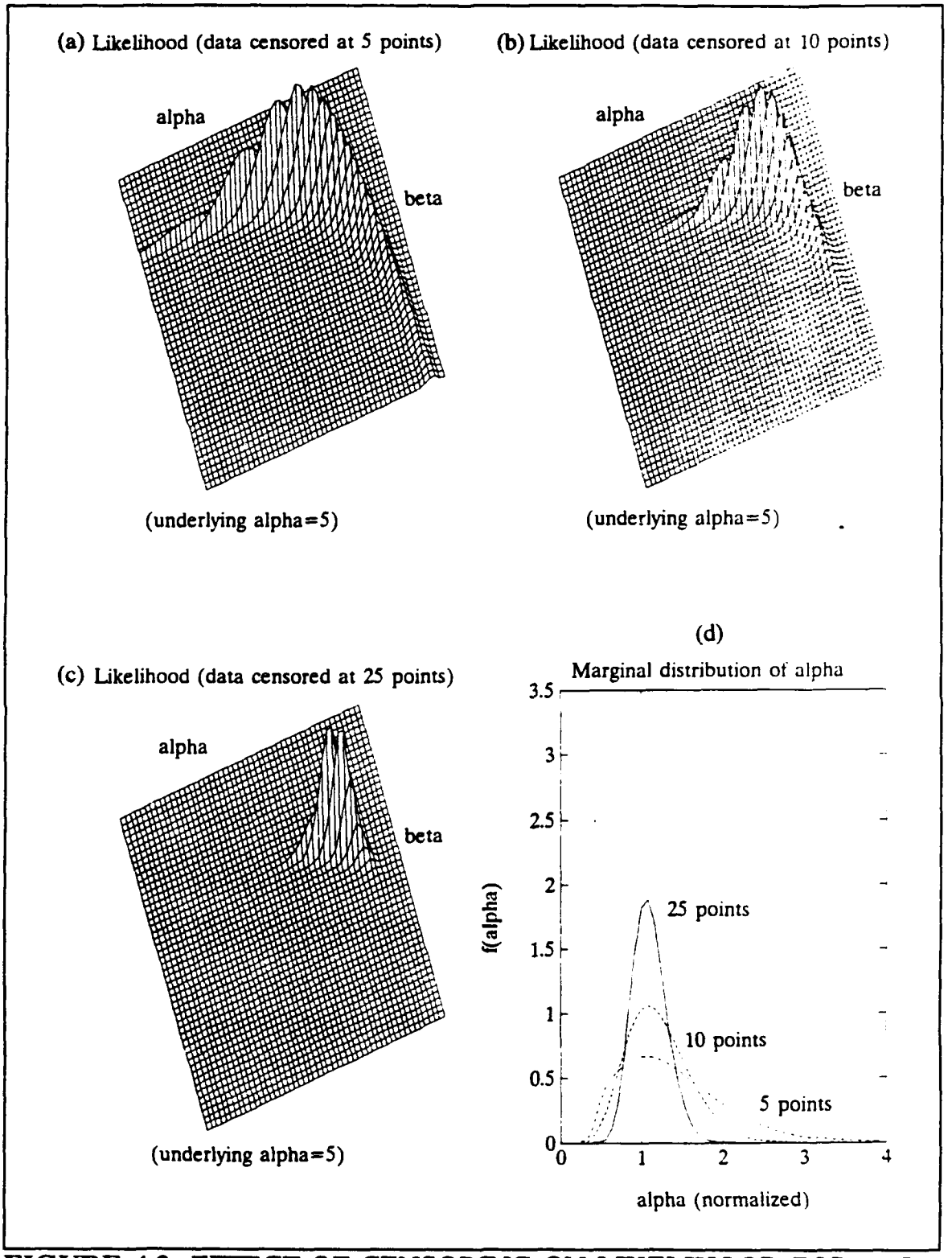

FIGURE 4.3 EFFECT OF CENSORING ON LIKELIHOOD FOR α=5

data possesses much less scatter than the previous data set described by α=0.2. The realizations of the data have less variability, resulting in narrowing the range of parameters which would be likely to fit the data. This is evident in the likelihood surfaces shown in Figures 4.2(a)-(c), and in the marginal distributions of α in Figure 4.2(d). The trend of reducing the range of the probable number of parameters as more data is realized is visible in the shapes of the likelihood surfaces. The likelihood surface of Figure 4.2(a) is that of only five data points. As illustrated by the 'L' shaped surface, the are many α and β combinations which would be equally likely. When more data points are obtained through delaying the censor (Figure 4.2(c)), the shape of the likelihood surface shrinks to a smaller number of probable parameters. The corresponding marginal distributions of each of these surfaces is provided in Figure 4.2(d). The significant reduction in the uncertainty in α is obtained by extending the experiment to achieve more realizations at higher values of the random variable. The observation in this case is that, for intermediate variability (α=1), censoring such a life experiment should be delayed.

The likelihood surfaces and marginal distributions of α for the data simulated for an underlying α=5 are shown in Figure 4.3(a)-(d). The

reduction of the probable pairs of parameters resulting from increasing the number of realized data prior to censoring is illustrated by the sharpening of the likelihood surfaces in Figures 4.3(a)-(c). The resulting marginal distributions of α show that a dramatic reduction of uncertainty in the parameters is obtained by letting the experiment continue in time vice censor early. The reason for this is that for $\alpha=5$, the failures will occur in a tighter range about the mean value, so that early failures really do not provide much detail about the characteristics of the data.

Figures 4.1 through 4.3 have shown that the number of realized data and the underlying shape parameter of the data have a significant impact on the nature of the uncertainty of the parameters, and therefore play a crucial role in determining a censor strategy. For large numbers of realized data, the likelihood surfaces will shrink to a spike about the underlying parameters, regardless of the scatter in the data, making the problem trivial. For the more realistic cases where there is only a small number of realized data, the knowledge gain for the estimated α is larger than for the estimated β when $\alpha<1$. If $\alpha>1$, however, the reverse is true. An explanation of this trend is achieved by referring back to the appearance of the distributions in the F^* domain. In the F^* graph, the parameter α is the slope of the line

representing the distribution, and the value of β is the location of intersection between the distribution and the horizontal line of $F^*=0$ (or F=.632). If $\alpha<1$, then the slope of the distribution in the F^* domain is less than 45°. For values of $\alpha<<1$, the distribution is nearly flat, and any variation of values along the F^* axis, caused by errors in the empirical rank of the data, would affect the value of β the most because it is the point of intersection of two nearly horizontal lines. For $\alpha>1$, the slope of the distribution in the F^* domain is greater than 45°. If $\alpha>>1$, then the distribution is a steep line, causing the rank error to effect the slope α more than β.

The design variable in planning an optimum censor strategy for an experiment is the censor locations, which are bounded by earliest censor of only one realization, and the latest censor would be after the last realization of the total N on test (the trivial case). If the available time of the experiment is insufficient to produce the required number of realizations of the random variable, or the test equipment is limited in capacity, then the total number of samples put on test must be increased by implementing censoring. The determination of the optimum censor location is made through the application of Information Theory.

B. USING CENSORING TO OPTIMIZE INFORMATION

A univariate objective function for maximizing the knowledge of the parameters is obtained through the application of information theory. As stated in Chapter 2, the information I is a scalar measure of how well the parameters are known. For convenience, Eq. 2.5 is restated as follows

$$I = \int p(\theta) \log p(\theta)\, d\theta \tag{4.2}$$

where $P\{\theta|D\}$ is the probability of the parameter, given a set of data. For large sample sizes, say $N > 1000$, the probability density of the parameters is asymptotically normal by the Central Limit Theorem

$$P(\theta) = \frac{1}{\sqrt{2\pi}\, b} \exp\left[\frac{1}{2}\left(\frac{\theta - a}{b}\right)^2\right] \tag{4.3}$$

and the information is analytically computable by

$$I = \frac{1}{\sqrt{2\pi}\, b} \exp\left[\frac{1}{2}\left(\frac{\theta - a}{b}\right)^2\right] \ln\left(\frac{1}{\sqrt{2\pi}\, b} \exp\left[\frac{1}{2}\left(\frac{\theta - a}{b}\right)^2\right]\right) \tag{4.4}$$

The typical sample sizes in engineering are $N < 100$, which does not produce a normal distribution of the parameters. As demonstrated by simulation, the marginal distributions of the shape parameters in Figures 4.1

through 4.3, the distributions are clearly not normal. The result is that an analytical form of the information *I*, such as that given in Eq 4.4, cannot be utilized. For small data sets, the probability density function of the parameter is the normalized likelihood function.

The likelihood function is useful because it contains the internal parameters of n, N, α, and β and has the advantage that it is not distribution specific. In developing an optimum censor strategy, the objective is to find the censor location x_c so that multiple repeated tests could be performed to maximize the certainty of the parameters, within the constraints of time and number of test stations. A high level of certainty in the parameters is characterized by a spike in the *likelihood* surface. On the contrary, a low level of certainty in the parameters would be represented by a more diffuse likelihood surface. The advantage of computing the information using the likelihood function is that it is a method of numerically distilling the many shapes of the likelihood surface into a single parameter.

The many shapes of the likelihood surface may be determined analytically by computing the 0^{th} moment, 1^{st} moment, 2^{nd} moment, and Kurtosis (mathematics of higher order moments). The drawback of using these methods is that the objective function would become multivariate due

to the number of moments which would be required to characterize the shape and the confidence on the estimator of the various moments cannot be defined.

The optimum censor foundation is established by simulation as previously illustrated in Figure 3.2. The simulation is conducted as if the model and parameters are known. The simulated data set $\{x_i\}$ is computed based on the expected rank of the i^{th} sample. The expected rank is defined as

$$F = \frac{i}{N+1} \quad , i = 1, 2, \ldots, N \tag{4.5}$$

The primary difference in this simulation for the calculation of information and previous simulations is that the data set $\{X\}$ was not computed based on a random ranking as occurrence in an experiment. Instead, the expected values of the data were computed from the expected rank. The reason for using the expected values is that the interest in this study is to determine the various trends of information for data sets possessing different amounts of scatter and the impact of censoring on the information. The use of random ranking would result in a large number of simulations required to be run before the desired trend would be clearly distinguishable.

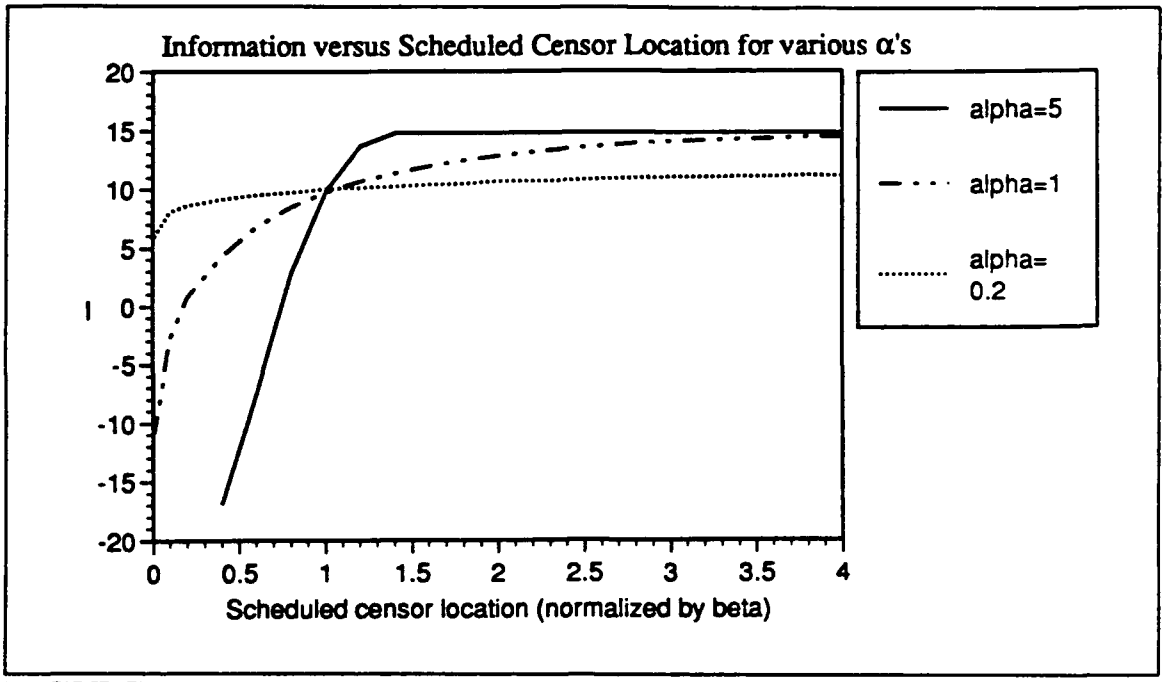

FIGURE 4.4 EFFECT OF α ON INFORMATION IN A SCHEDULE CENSORED EXPERIMENT

Once the simulated data set is obtained, the number of realizations, n, is determined based on the number of x_i's which have values less than the censor value x_c. The information *I* is then computed based on the n realized data and N-n censored data. The repetitive computation of *I* for various censor strategies and different sets of data makes it possible to determine the best x_c for increasing *I*, and to evaluate when a point of diminishing return is reached when trying to improve *I*.

The simulations conducted in this study are based on a life test experiment on sets of data described by three shape parameters: $\alpha = 0.2, 1,$

and 5 for the reasons discussed in Chapter III. The impact of both scheduled censoring and censoring by the number of realizations was investigated. The algorithms and software used in this simulation are provided in Appendix D.

The graph shown in Figure 4.4 is a comparison of the effects of the underlying value of α for the data on the information I for scheduled censoring. The time of censor axis is normalized by the underlying location parameter β so that the time of the censor relative to the mean life is evident. The curve representing α=0.2, or data with a large amount of scatter, appears nearly flat. The only dramatic changes which occur for this curve are in the region of very early censor times. Therefore, the small amount of increase in the information of the parameters which results from allowing the experiment to continue without censoring is not justifiable. The increase in I for α=1 occurs rather quickly up to the mean life and then diminishes. This is due to the increased grouping of the data and the observation that fewer failures occur early, resulting in little information being gained for early censor times. The change in information is even more dramatic for the case where α=5. The data is more grouped about the mean, so that the information gain occurs only in this area.

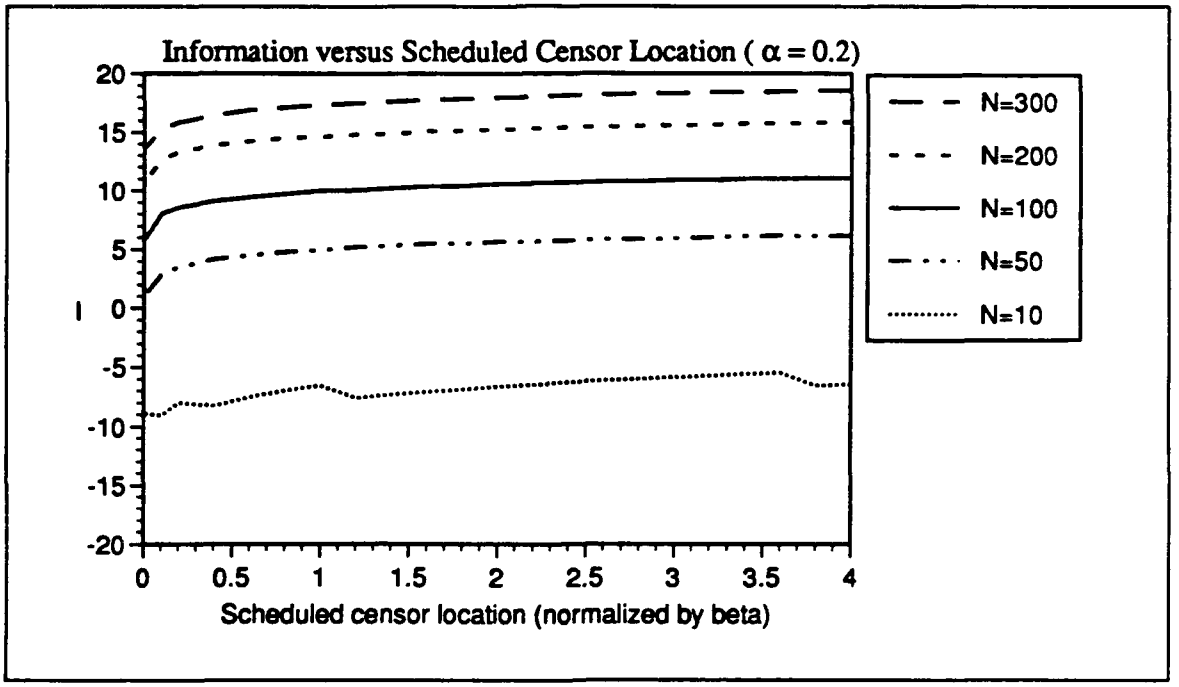

FIGURE 4.5 EFFECT OF N ON INFORMATION IN A SCHEDULE CENSORED EXPERIMENT FOR α=0.2

Figure 4.5 is a graph of information versus the scheduled censor times for various sizes of data sets for α=0.2. The purpose of this graph is to evaluate the impact of increasing N on the information. As shown in the graph, the increase in *I* is dramatic between N=10 and N=100 samples. Note, however, that the increase in *I* for an increase from N=100 to N=300 samples is significantly less. The important implication of this graph is that there exists a point of diminishing return in trying to increase *I* by obtaining more data, and that the amount of increase is quantifiable. Similar results were obtained for α=1 and α=5, as shown in Figures 4.6 and 4.7.

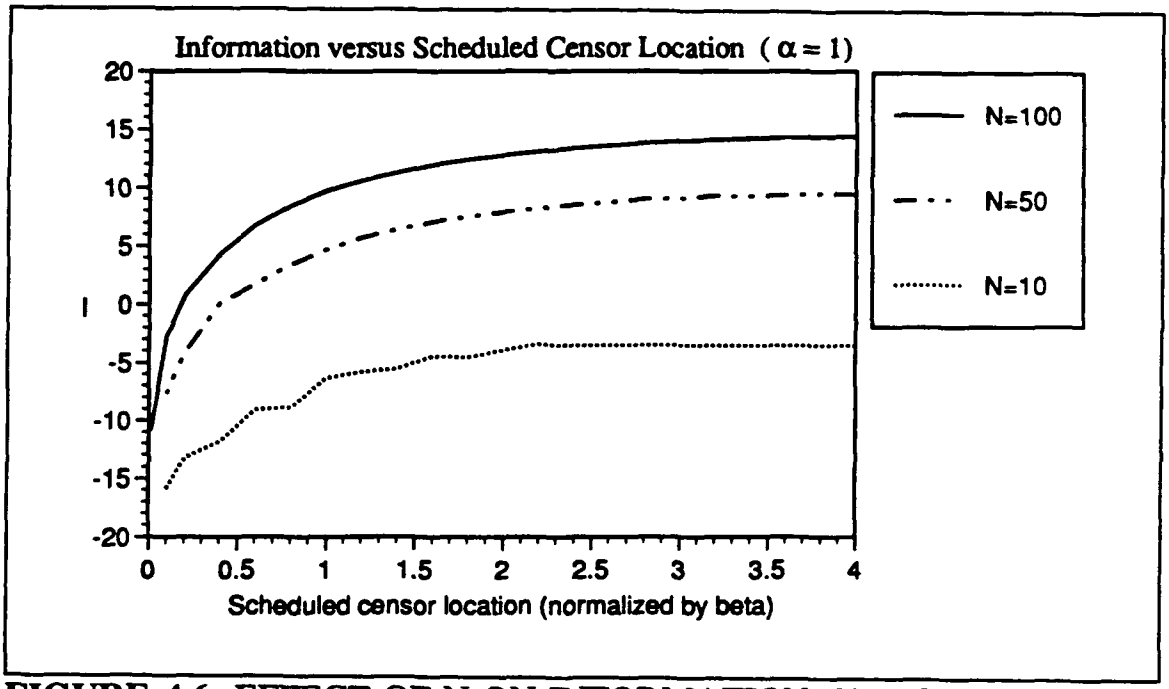

FIGURE 4.6 EFFECT OF N ON INFORMATION IN A SCHEDULE CENSORED EXPERIMENT FOR α=1

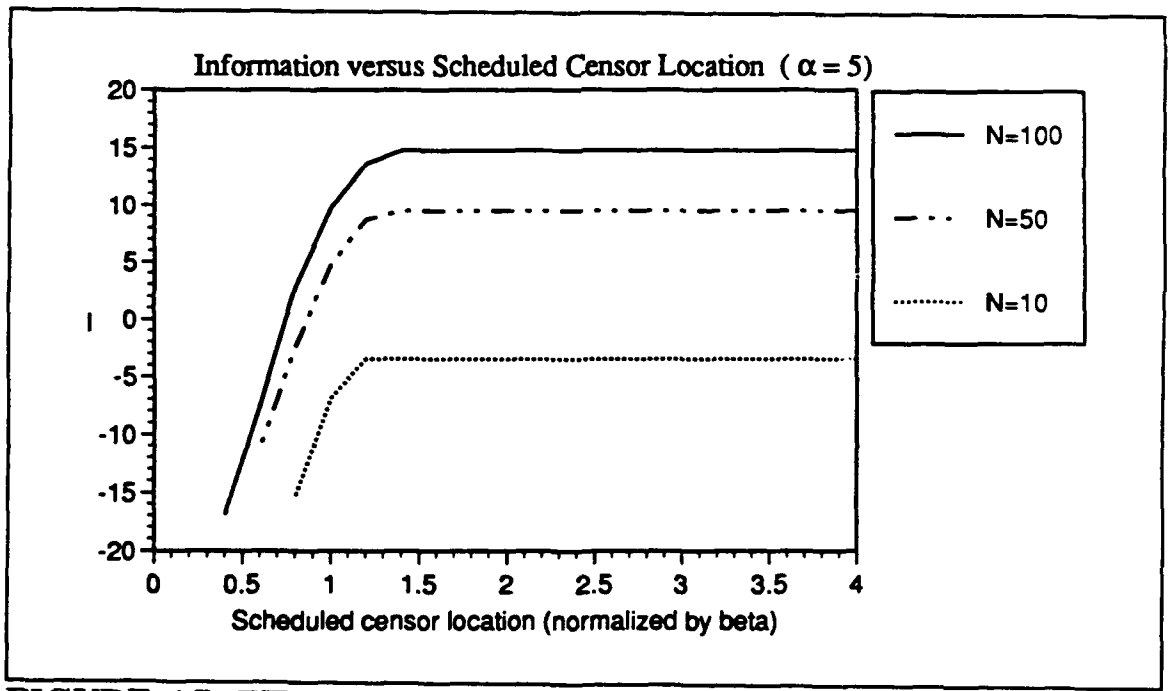

FIGURE 4.7 EFFECT OF N ON INFORMATION IN A SCHEDULE CENSORED EXPERIMENT FOR α=5

The effect of censoring a experiment based on the number of realized data on the information is shown in Figure 4.8 for various underlying shape parameters. The abscissa is labelled the number of fractional realization because the number of realizations has been normalized by the number of samples put on test. The value of 0.1 for the fractional number of realizations means that 10% of the samples tested have failed. The plot of the curve for α=0.2 appears initially flat and then begins to increase at a fairly constant rate. This is due to the long, tunnel like shape of the likelihood surface for small number of data points when $\alpha < 1$, as was shown in Figure 4.2. The implication of this shape was previously

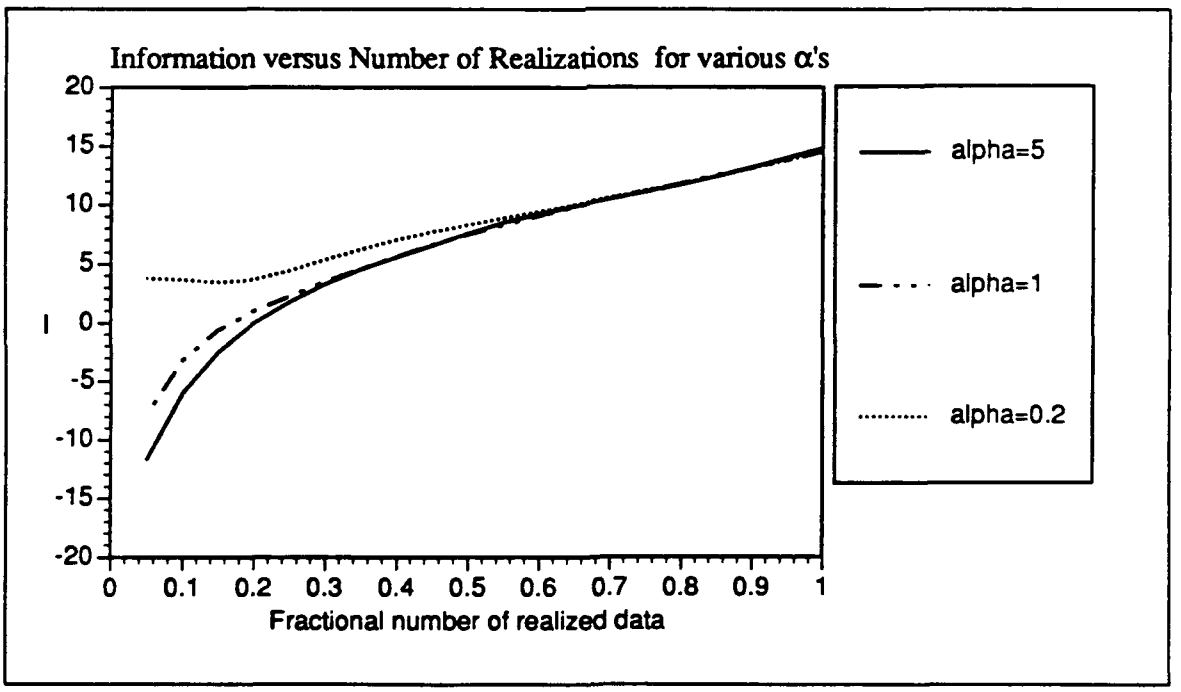

FIGURE 4.8 EFFECT OF α ON INFORMATION FOR AN EXPERIMENT CENSORED BY THE NUMBER OF REALIZATIONS

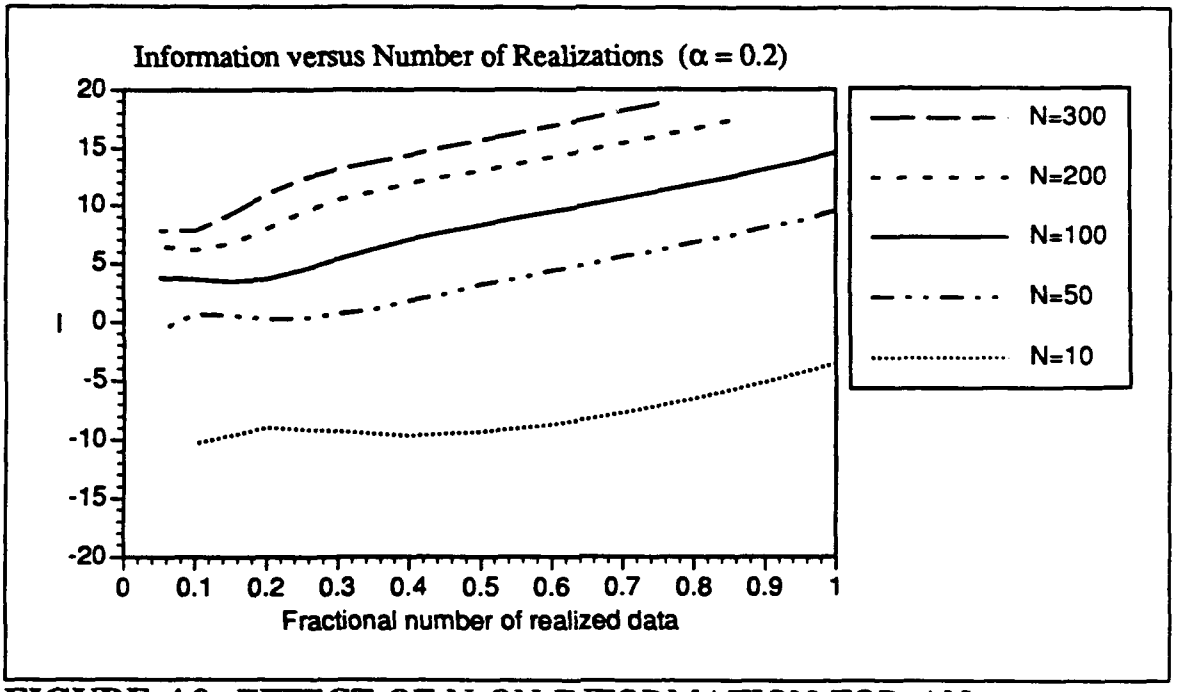

FIGURE 4.9 EFFECT OF N ON INFORMATION FOR AN EXPERIMENT CENSORED BY THE NUMBER OF REALIZATIONS FOR α=0.2

disscussed and is caused by the large number of location parameters which would be likely to fit the data. Due to constraints imposed on the numerical algorithm to integrate the volume of the likelihood surface, the upper limit for integration in β was approximately 20 times the underlying value. The curve is flat in the region of fractional realizations less than 0.2 because the slight changes which occur in the shape of the surface take place past the maximum β integration limit, and are therefore not detectable. The justification for establishing this upper limit in β is that changes which occur

in the likelihood surface past the point of 20 times the mean life of an object are of little practical use.

The curves representing α=1 and α=5 in Figure 4.8 begin at lower values of *I* and increase faster than for α=0.2. The reason the information is initially higher for small values of α is that the curves representing the probability density f(x) for the Weibull model are skewed toward the region of early failures. As the value of α gets larger, the density becomes narrower (less scatter) and less skewed toward the early failures. Therefore, early failures which occur when α is large do not provide much information about the underlying shape parameter.

Figures 4.9 through 4.11 are graphs which show the influence of the total N samples put on test on the information for the three α's of concern. In each figure, the concept of a point of diminishing return in improving I by more data is validated.

1. Optimization of Information in a Time Limited Experiment

An illustration of how recursive censoring can be used to improve the information of the parameters is provided in Figure 4.12. This figure is a plot of I versus the number of fractional realizations for α=0.2 for N=10, 50, and 100 total samples tested. Note that on the top of the graph an

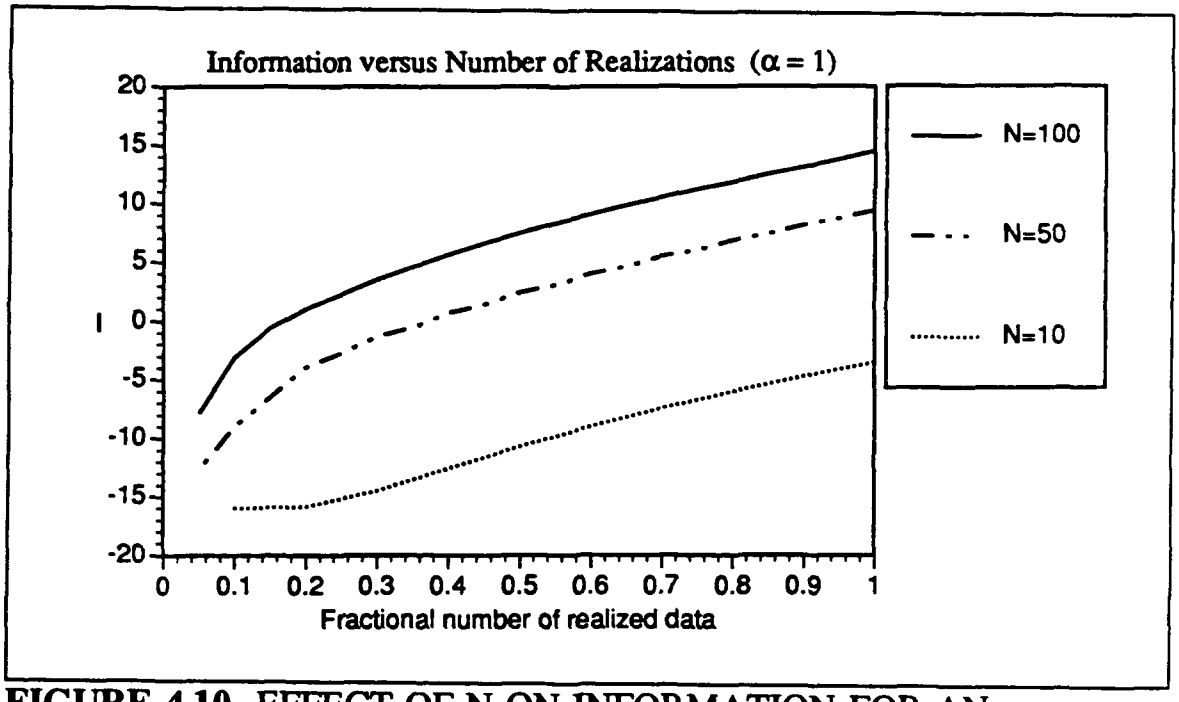

FIGURE 4.10 EFFECT OF N ON INFORMATION FOR AN EXPERIMENT CENSORED BY THE NUMBER OF REALIZATIONS FOR α=1

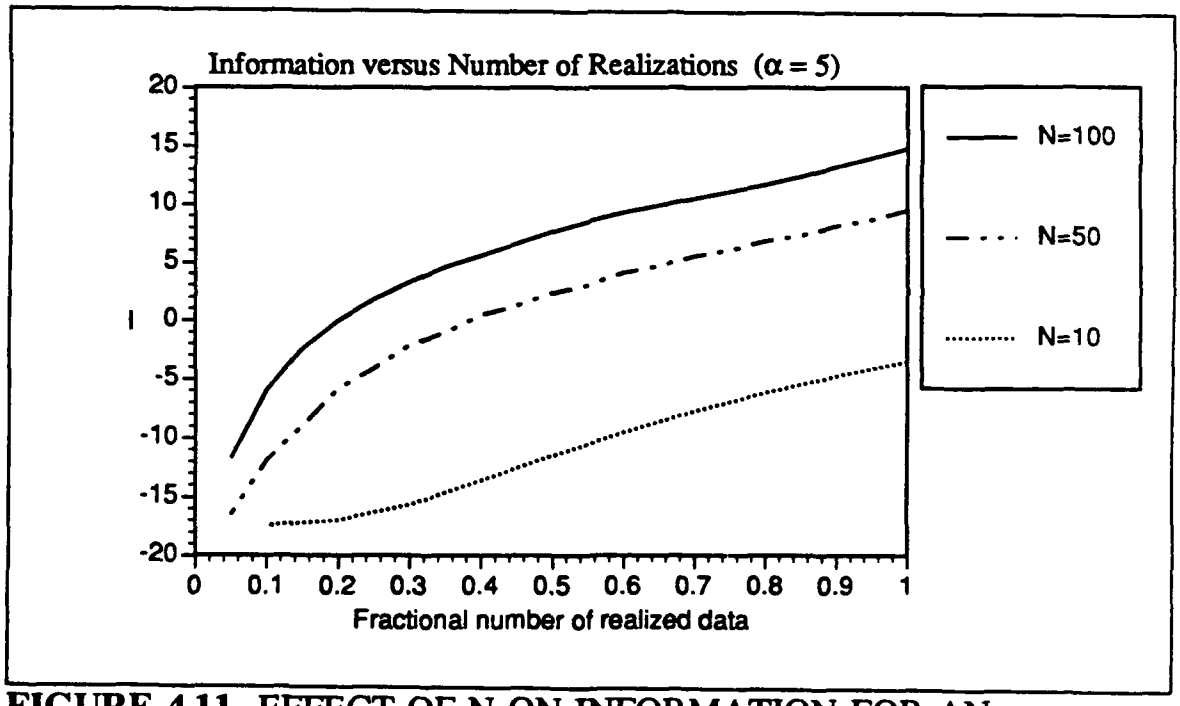

FIGURE 4.11 EFFECT OF N ON INFORMATION FOR AN EXPERIMENT CENSORED BY THE NUMBER OF REALIZATIONS FOR α=5

additional axis of scheduled censor times is plotted which is used to indicate the fractional number of samples realized within the specified time prior to censoring. The scheduled censor time of 0.1 of the mean life corresponds to the point of approximately 46% of the samples realized on the fractional number of realizations axis. An example of the impact of an early censor on the information of the parameters is shown on the figure. In this example, suppose that two sets of life tests of 50 samples were initiated at the same point in time. One test was allowed to progress through the duration of time up to four times the mean life, without censoring. The other test are censored at 10% of the mean life, and immediately 50 more samples were put on test. The point of the scheduled censor at 0.1 establishes the baseline to be used in the comparison of the information between the two tests.

The quantity labeled I_1 is the increase in information which results from the test proceeding to 0.2 of the mean life, without censoring. As shown on the graph, the amount of increase is extremely small. For the test which was censored, however, a total of 100 samples were put on test for a period of time of 0.1 of the mean life. The increase in information is labelled as I_2 and represents a drastic increase in the information. Even more

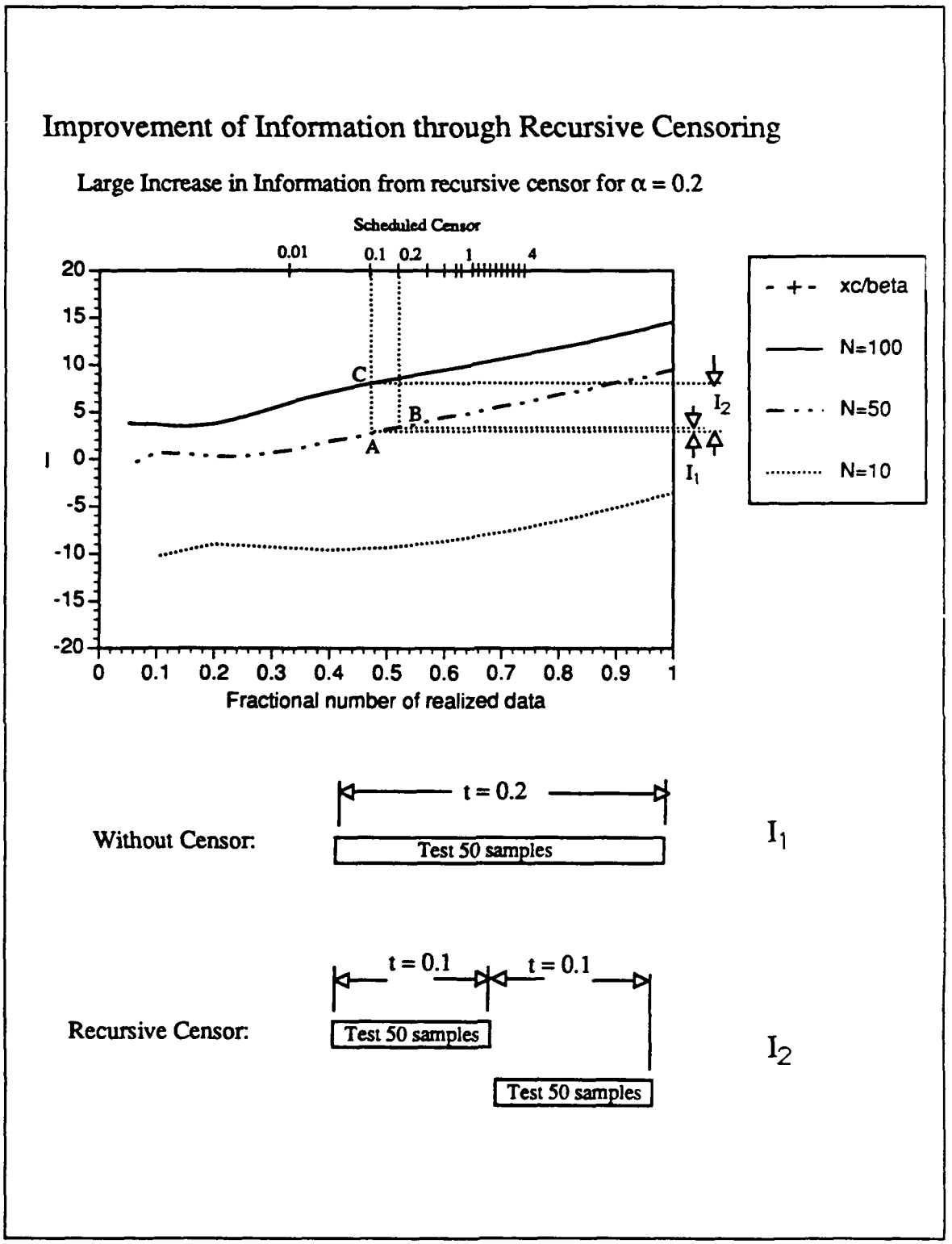

FIGURE 4.12 INCREASING INFORMATION THROUGH EARLY CENSORING IN AN EXPERIMENT

important is that the I_2 is a larger increase in information than would have occurred if the test without censoring was allowed to continue up to four times the mean life. The significance of this is that more information about the parameters was obtained in a fraction of the time it would take if no censoring was utilized.

2. Optimization of Information in a Capacity Limited Experiment

Information theory can also be applied to an experiment which is limited by the capacity of the test equipment. Consider an example in which the goal of a particular experiment is to predict the reliability of a large flat plate, such as the decking on a ship. The problem exists that the test equipment available only produces 40% of the expected mean failure load of the plate. Resolution is required for the question of whether the appropriate parameters can be obtained by testing the full size plate. The issue is resolved through the application of information theory. The goal is to use information theory to determine if an experiment will produce better certainty of the parameters by testing smaller scaled down sizes of the plate or simply more tests of the big plate.

The failure process of the plate is modeled by dividing it up into many smaller, equal-width strips of plate in parallel. If the failure process

$$R(p_i) = \exp\{-(\frac{p_i}{\beta_l})^{\alpha}\} \qquad (4.6)$$

is characterized by fracture mechanics, the entire plate will fail when a crack is initiated at the weakest strip and propagates through the plate catastrophically. The Weibull model is selected for this problem because it is the presence of a extreme value which results in the failure. Reliability for an individual strip of the plate is given as

where: p_i is the random variable of load for the i^{th} strip
β_l is the mean load of failure for each strip
α is the shape parameter of the failure model
$R(p_i)$ is the reliability for the value of the random variable.

Since the process is weakest link (or one which is serial in the failure mechanism) the reliability of the plate is the product of the reliabilities of the individual strips in the plate as in

$$R = R(p_1)\ R(p_2)\ \ldots\ R(p_k) \qquad (4.7)$$

Three different sizes of the plate are proposed to be tested utilizing the maximum load of the test machine. The largest size tested is chosen to be the full size plate, because no size effect considerations are required. The two smaller sizes, one representing a moderate reduction in the size of the plate (medium plate), and the other representing a large reduction in size

(small plate), are determined from size effect considerations and the desired number of failures in the experiment.

The three proposed plates to be tested are shown in Figure 4.13. The values of k_L, k_M, and k_S represent the number of parallel strips in the plates; a unitless metric of the plate width since all strips are assumed to have both

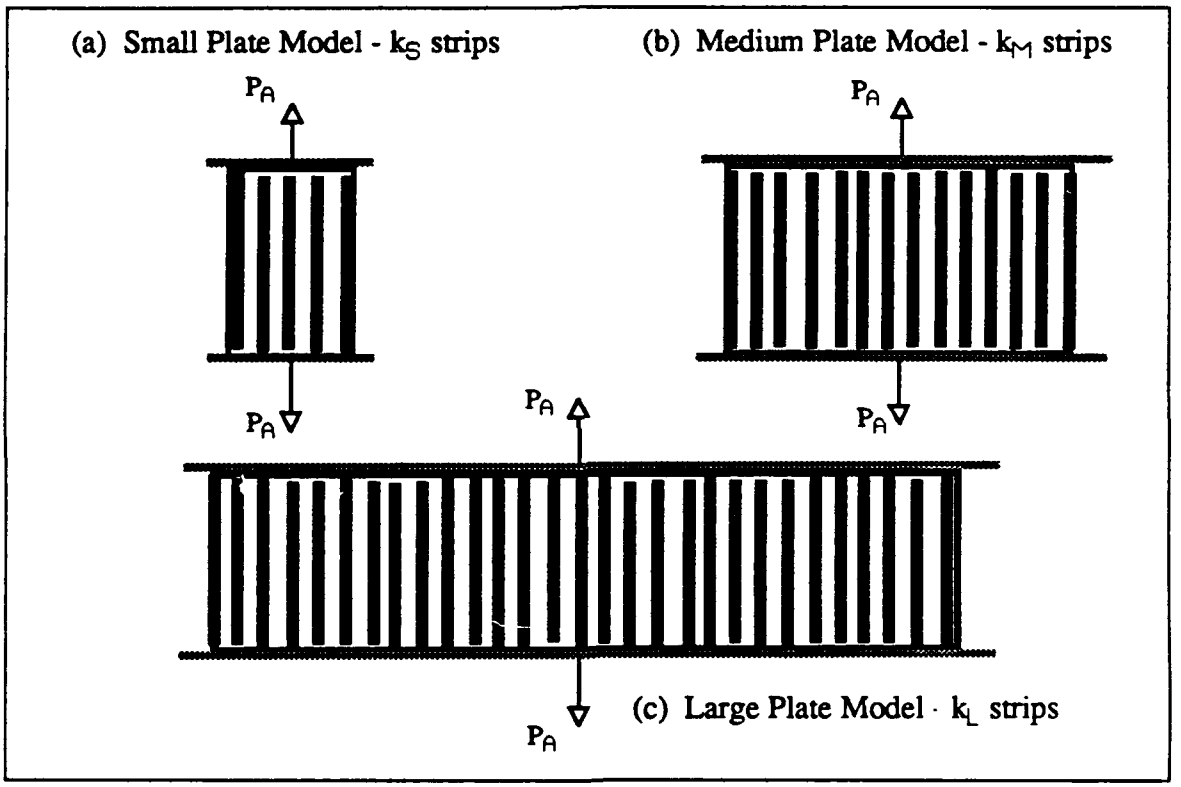

FIGURE 4.13 FAILURE MODELS FOR A PLATE IN TENSION

equal width and length. The reliability of the entire large plate is obtained from Eq 4.7 by taking into account equal loading for each strip and the

presence of k_L strips

$$R_L = \left[\exp \left\{ - \left(\frac{P_a}{\frac{k_L}{\beta_l}} \right)^{\alpha} \right\} \right]^{k_L} \tag{4.8}$$

Similar expressions are obtained for the reliability of the medium and small plate. The intention is to select the proper sizes of the medium and small plate such that the reliability of these smaller plates is equal to the reliability of the large plate. This makes it possible to predict the reliability of the large plate by testing one which is smaller. In equation form, this is represented by equating the respective reliabilities: $R_L = R_M = R_S$. These equations are then simplified in terms of the applied load p_i and the number of s. ps in the test sample k. The resulting equations are written as

$$\frac{p_M}{p_L} = \left(\frac{k_L}{k_M} \right)^{\frac{1}{\alpha}} \tag{4.9}$$

$$\frac{p_S}{p_L} = \left(\frac{k_L}{k_S} \right)^{\frac{1}{\alpha}} \tag{4.10}$$

Changes in the sizes of the plate do not affect the intrinsic scatter in the failure data because the failure is governed by the weakest link. Therefore, the values of shape parameters of the three plates are assumed equal: $\alpha_L = \alpha_M = \alpha_S$. The difference in the sizes affects the mean value of the strength since there is a greater likelihood of possessing a very weak strip when the number of strips in the plate is large. Fortunately, the increase in the number of strips in the structure reduces the individual loads on each strip because the load is more distributed.

Two different load levels, p_M/β_1 and p_S/β_1, were established for the medium and small plates which would produce failures in 60% and 90% of the samples tested, respectively. These percentages were selected in order to determine the influence of the numbers of failures for the smaller plates on the information of the parameter α. The loads which correspond to these probabilities of failures $F(p/\beta_1)$ are determined from the CDF of the failure model which is computed using the expected values of the parameters. In many applications in engineering, some knowledge is possessed about the expected shape and location parameters of the failure model. It is assumed in this example that the underlying $\alpha = 5$, $\beta = 1$. A plot of the resulting CDF is provided in Figure 4.14. Based on this curve, the capacity limited

load placed on each strip in the large plate is $p_L/\beta = 0.4$, which corresponds to failure of 2% of the samples tested. The size of medium plate is selected to produce 60% of the plates tested to fail, or $p_M/\beta = 0.97$ from Figure 4.14. The small plate is to be sized such that 90% of the plates tested will fail, resulting in $p_S/\beta = 1.2$. The purpose of choosing those particular loads is to determine which plate should be tested so that the most information about the parameters is obtained from the experiment.

Determination of the sizes of the medium and small plates relative to the large plate is obtained by substituting the corresponding loads discussed above in Eqs 4.9 and 4.10 for $\alpha=5$. The result is that k_L is 83.86 times larger than k_M, and 243 times larger than k_S.

The graph of the Information *I* versus the number of fractional realizations for a process with an underlying value $\alpha=5$ is provided in Figure 4.15. In the case of the large plate, the probability of failure is so low at the load at maximum capacity that the number of plates tested was chosen to be large, or N=100. The information resulting from testing 100 large plates is labelled by point 'A' in Figure 4.15. If the medium plates are tested a higher percentage will fail, so only N=50 are tested. This increases the information dramatically, as seen by the point labeled 'B.' If 10 of the

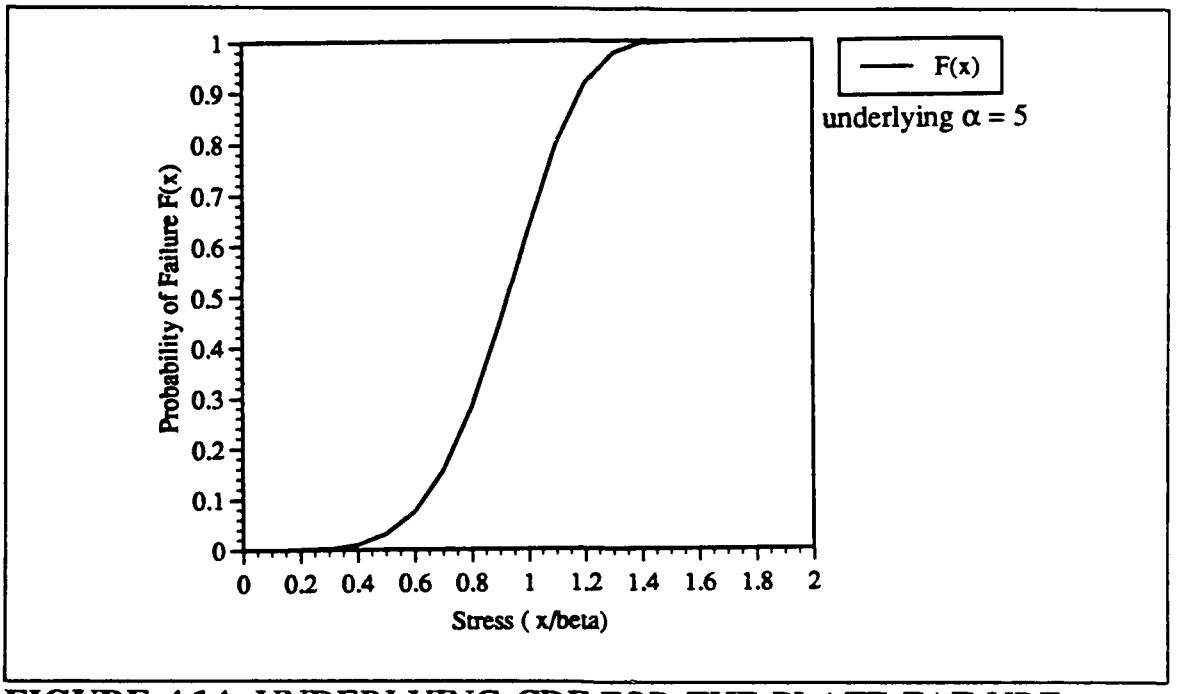

FIGURE 4.14 UNDERLYING CDF FOR THE PLATE FAILURE EXAMPLE

small plates are tested, almost all samples will fail, producing the information labeled 'C' in Figure 4.15. If 50 of the small plates are tested, the information is increased further to point 'D.'

The purpose of performing this capacity limited experiment is to determine the parameters of the failure model of the large plate so that the reliability at various stresses may be quantified. Testing the large plate, however, only produces a few failures due to the limited load. The result is a very small amount of information I on α. The size of the plate can be reduced to a size which is sufficiently small such that all samples which are

Minimizing the Loss of Information in a Capacity Limited Experiment

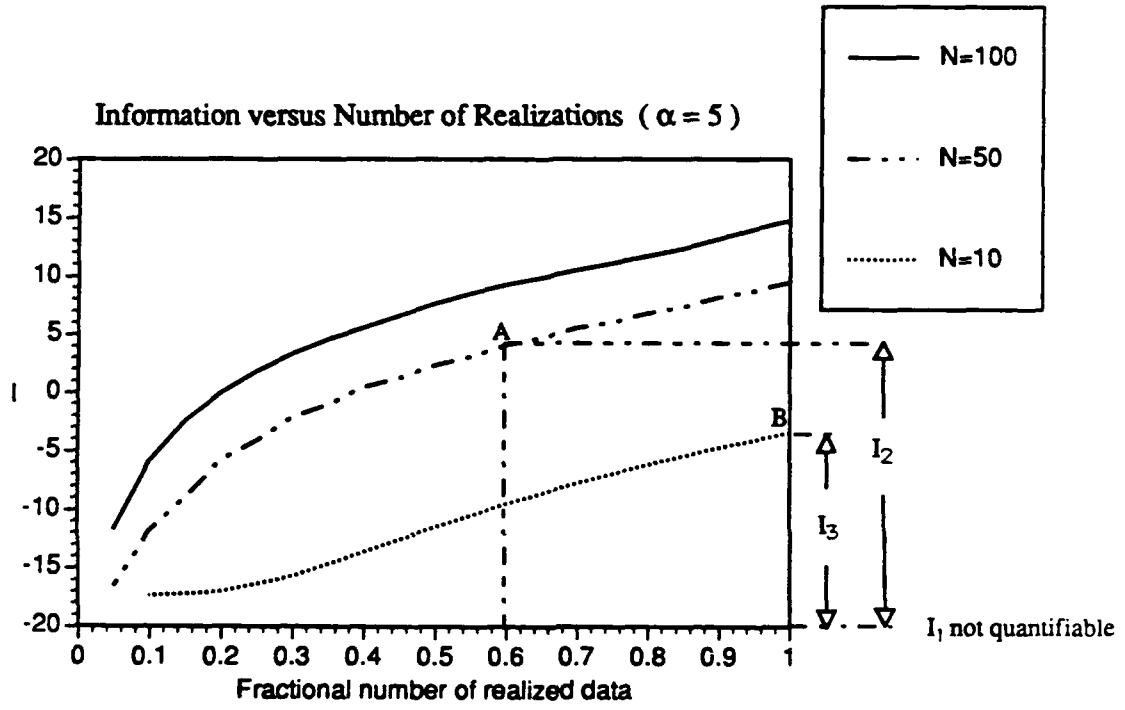

I_1 : Information gain if Full scale shaft tested

I_2 : Information gain if Half scale shaft tested

I_3 : Information gain if Tenth scale shaft tested

FIGURE 4.15 MINIMIZING THE LOSS OF INFORMATION IN A CAPACITY LIMITED EXPERIMENT

tested will fail. The small size of the samples makes it possible to test a large number of plates to failure, but the gain of information on α diminishes once a sufficient amount of data has been collected. The number of samples tested for the small size can be optimized to maximize the information on α.

The uncertainty, however, is reintroduced from the size effect when the information on α is transformed from the small sample back to the actual size. This is due to a large k_L/k_S ratio being raised to the exponent of $1/\alpha$. Any uncertainty in the α will produce a substantial error in the predicted location parameter of the large object. What is gained, therefore, in the knowledge of α by testing more small samples may be lost in the transition to the actual sample because of the large size effect.

Increasing the size of the sample tested will reduce the impact of uncertainty of α, but the information of α may be lower than that obtained from testing many of the very small samples. The objective then is to minimize the loss of information by increasing the size of the sample in order to reduce the impact of uncertainty in α on a large scaling effect ratio. In this regard, point 'B' in Figure 4.15 would be the desired target point for the design of the experiment.

V. CONCLUSIONS

The characterization of reliability requires a failure model based on the physics of the failure process, and parameters based on experimental data. The limitations of experiments in terms of time or capacity give rise to the need for an experiment designed to maximize the knowledge of the parameters within the constraints of the limitations. The optimality parameter used was the information I of the parameters which distills the multitude of shapes of the likelihood surfaces into a single parameter.

This study has demonstrated that for high variability data, such as life or fatigue data, the information obtained from experiments can be dramatically increased by recursive censoring. In cases of low variability data, such as data resulting from experiments limited in capacity, information can be used to determine the maximum structural dimension which would result in meaningful estimation of the parameters.

Due to the large number of possible shapes in the likelihood surface, an integration scheme which accommodates an adaptive mesh requires development. This would provide the ability to compute information for a

large range of parameters without first having to define the bounds of the likelihood surface for every data set.

The application of information theory developed in this study should be extended to cover a range of parameters describing the randomness of data and censoring strategies in order to develop a set of optimality curves which could be used in interactive planning of an experiment design.

APPENDIX A: RANK AND ORDER IN A DATA SET

The order of a data set is the arrangement of the data from the smallest magnitude of the realized random variable to the largest. An ordered data set satisfies the following inequalities [Bury, 9]

$$x_1 \leq x_2 \leq \cdots \leq x_n \tag{A.1}$$

The rank of a particular sample value x_i with respect to the other values within the data set is determined by its relative magnitude. The smallest value, or the first value in the ordered data set, would have the lowest ranking, and conversely, the largest value would have the highest ranking. There are numerous ranking methods available which provide discrete values of the CDF based on the ranking of each sample in the data set. One of the more widely accepted methods of determining F is that of expected rank

$$F(x_i) = \frac{i}{N+1} \qquad i = 1, 2, \ldots, N \tag{A.2}$$

where $F(x_i)$ is the probability that a value at least as large as x_i will occur in a data set {X} of N samples. Since the value $F(x_i)$ can be determined

without the selection of a model, the expected rank of an ordered data set represents a viable nonparametric method in computing reliability.

For example, a fiber having a rank of 0.25 is at least as strong as 25% of the fibers tested, which is the same as saying that the probability failure F=0.25. However, it may subsequently be determined from additional testing that the particular fiber is only as strong as 20% of the fibers tested, or F=0.2. Since all fibers cannot be tested, the true rank of the fiber will never be known, but the rank serves as a useful way of estimating the value of F so that the data may be plotted.

APPENDIX B: LIKELIHOOD AND MAXIMUM LIKELIHOOD ESTIMATORS

The likelihood function is defined [Bury, 9] as

$$L(X;\theta) = \prod_{i=1}^{n} f(x_i;\theta) \tag{B.1}$$

where: $L(X,\theta)$ is the likelihood of the parameter(s) θ given the data set X

$f(x_i,\theta)$ is the pd of the i^{th} realization of x for the parameter(s) θ

n is the number of samples in the data set.

The symbol θ used in the equation is a vector which represents both the shape and location parameters α and β used in the Weibull distribution. Recall that the pdf is the derivative of the CDF with respect to the random variable, which is given as follows for the Weibull distribution

$$f(x;\alpha,\beta) = \frac{\alpha}{\beta}\left(\frac{x_i}{\beta}\right)^{\alpha-1} \exp\left[-\left(\frac{x_i}{\beta}\right)^{\alpha}\right] \tag{B.2}$$

The likelihood function is a mathematical representation of the probability that a selected pair of parameters describe a given data set. A large value of likelihood results when the selected parameters are more likely

to be the underlying parameters. This is due to the product of the probability densities. If the selected parameters are far from the underlying values, the resulting probability densities will be very small numbers, and the product of these numbers will be an even smaller number. As the selected parameters are in the neighborhood the underlying values, the probability densities will become larger, and correspondingly, the likelihood will become larger. The point at which the likelihood is the maximum represents the most likely parameters which describe the given data set, and are referred to as the maximum likelihood estimators (MLE). The MLE parameters can be determined by calculus by taking the derivative of likelihood function of equation (B.2) with respect to the parameters θ. The resulting MLE parameter for the Weibull distribution are given as

$$\alpha = \frac{1}{\left[\dfrac{\sum_{i=1}^{n} x_i^{\alpha} \ln x_i}{\sum_{i=1}^{n} x_i^{\alpha}} - \dfrac{1}{n} \sum_{i=1}^{n} \ln x_i \right]} \tag{B.3}$$

$$\beta = \left[\frac{1}{n} \sum_{i=1}^{n} x_i \right]^{\frac{1}{\alpha}} \tag{B.4}$$

Alternatively, the values of likelihood for a model consisting of two parameters, such as in the Weibull model, can be represented as a three-dimensional surface plot or two-dimensional contour plot. The likelihood surfaces and contour plots for the data sets represented by curves in Figure 3.3 are given in Figure B.1. For the cases where the likelihood surface is unimodal, the MLE parameters (determined by Eqs. (B.3) and (B.4)) are in accord with the peaks on the likelihood contours.

The estimators determined either by the likelihood contour or by MLE are based on the given data set. Due to the randomness associated with each set of data, different estimators are likely to be obtained from different sample sets, even from the same population.

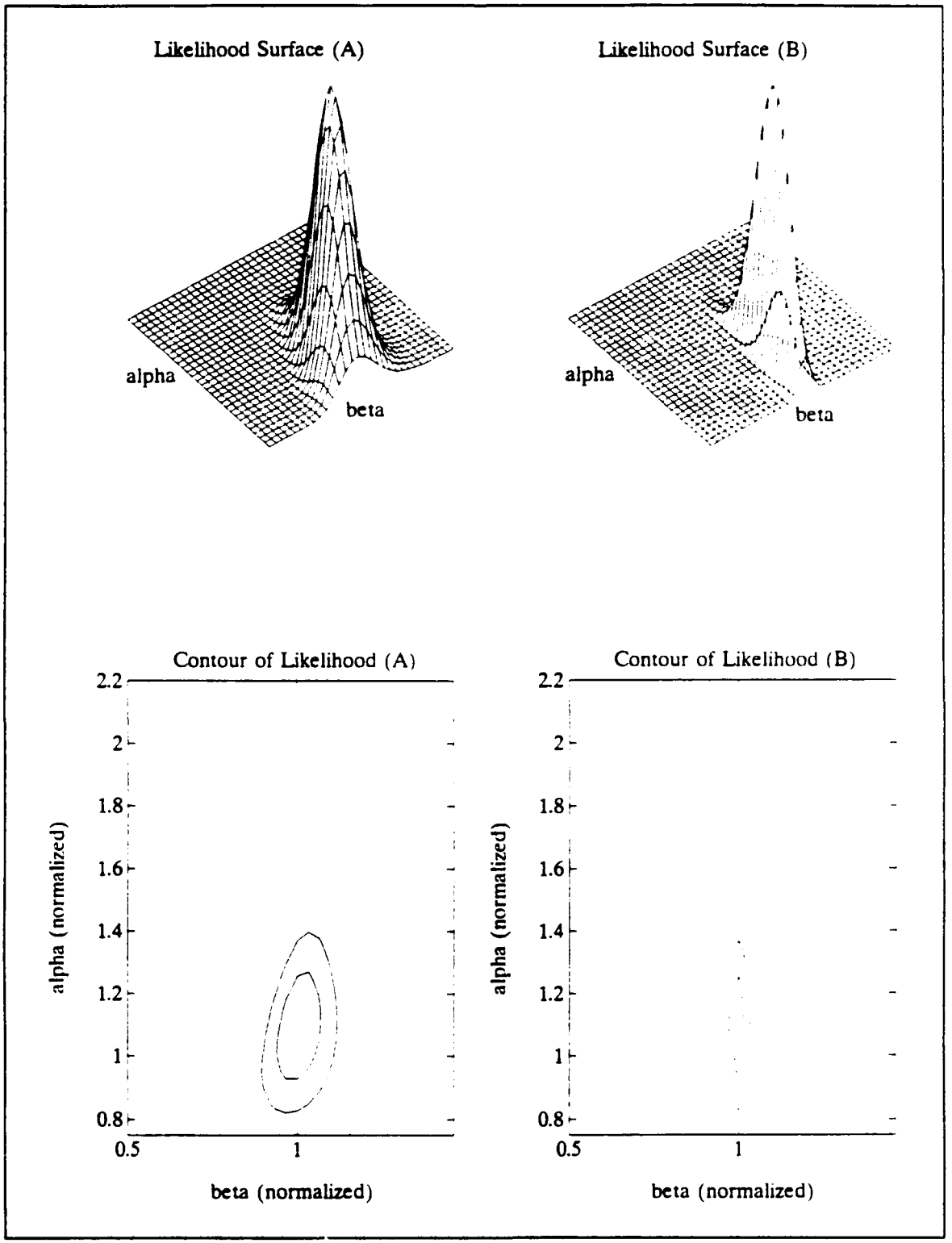

FIGURE B.1 LIKELIHOOD SURFACES AND CONTOUR PLOTS FOR TWO DATA SETS

APPENDIX C: LOWER TAIL SUBTLETIES IN DATA

As an illustration of the many subtleties in the lower tails of the distributions encountered in random data sets, four representative F^* curves are provided in Figure C.1. These plots were obtained from randomly generated sets of data of 100 samples. The underlying distributions which are straight lines are plotted as a guide for comparison. Notice that in some cases the points fall above the line, indicating data which fail earlier than the model, while in other cases the points fall below the lower portion of the curve, indicating that the samples later than the model. There will, of course, be cases in which the data closely resembles the underlying distribution. The utility of displaying the distributions in the F^* domain is clearly evident in these four graphs.

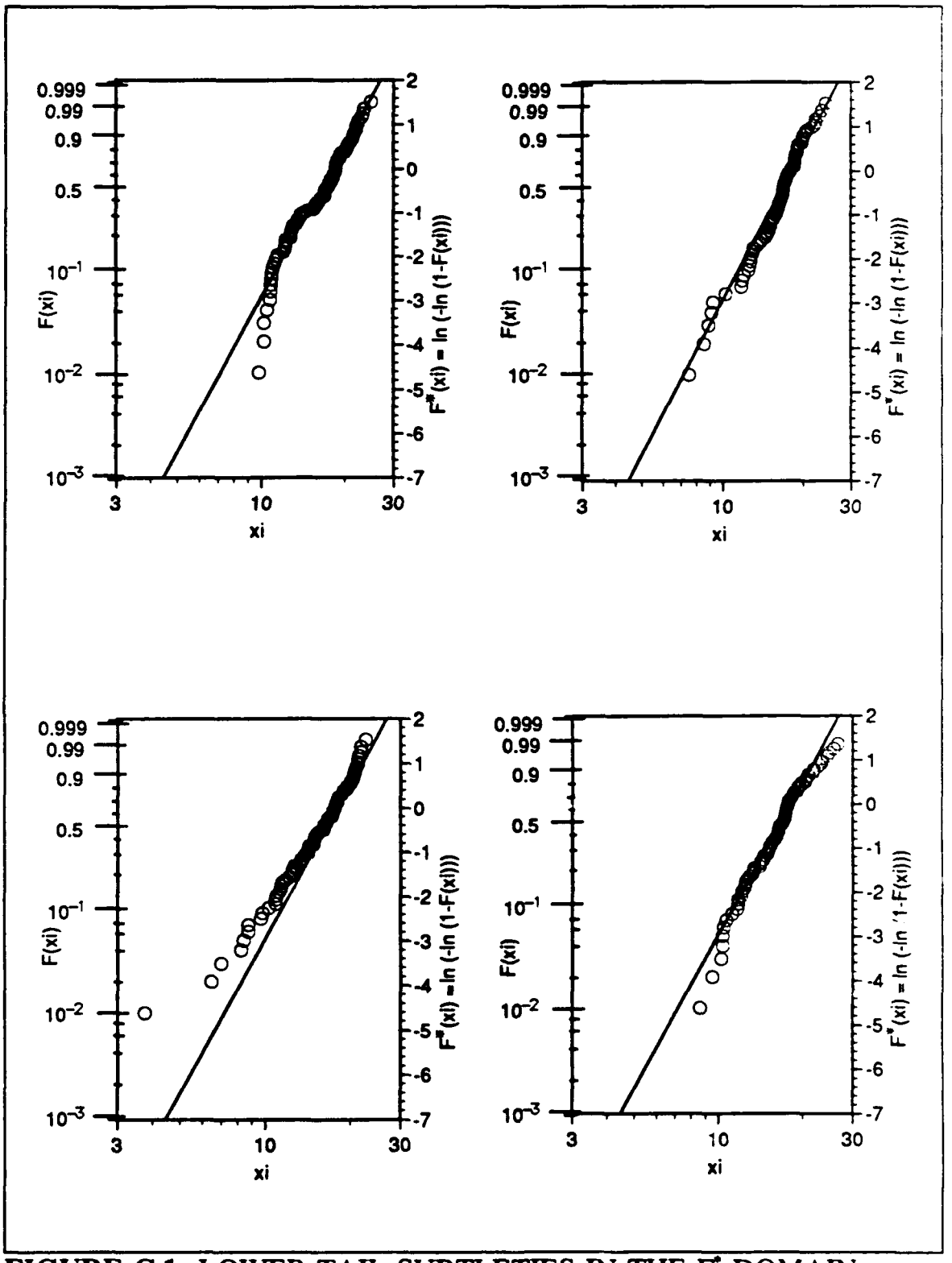

FIGURE C.1 LOWER TAIL SUBTLETIES IN THE F* DOMAIN

APPENDIX D: SIMULATION SOFTWARE

I. SOFTWARE DESCRIPTION

The purpose of this appendix is to provide a description of the simulation procedures and the software. The rationale behind each simulation procedure implemented will be addressed in this appendix, followed by the software used to implement that particular component. The software programming used in the simulation was developed using the MATLAB program by The MathWorks, Inc.

A. SIMULATION USING A NONPARAMETRIC METHOD TO CHARACTERIZE RELIABILITY

This simulation was an investigation into whether practical levels of reliability (i.e., 0.9999 or 0.99999) could be achieved without the need of a model. The advantage of using a nonparametric method is that reliability can be quantified based on the data directly, without the need of fitting a particular distribution to the data. The issue to be determined from the simulation is whether or not using a nonparametric method is pragmatic in

the amount of data required and the associated cost and time to obtain the data.

The quantity which is random in any experiment is the probability of occurrence of a random variable. In terms of composite reliability, it is the probability of failure in the random variables of strength and life which is random. This random probability of failure can be simulated by setting it equal to a random number, defined as having a value between zero and one, generated by a computer program.

The data which correspond to those probabilities of failure can be computed using an empirical rank of the data. The concepts of order and rank of data are discussed in Appendix A.

1. Simulation Description

A set of numbers representing the probability of failure $F(x_i)$ of N samples is generated as a set of random numbers {F}. The data set {X} cooresponding to those values of {F} are computed using the Weibull distribution with known shape parameter α and location parameter β

$$x_i = \beta \left(-\ln(1 - F(x_i))\right)^{\frac{1}{\alpha}} \qquad \text{(D.1)}$$

The data set {X} represents a set of realized random variables such as strength or life, which have underlying values of the parameters α and β that describe the data set. In other words, {X} simulates an actual set of data that would have been obtained by testing a structural sample, fiber or composite, to failure. The difference in the simulated data set {X} and a data set resulting from an actual test is that the underlying parameters are known for {X}.

The data set {X} is then ordered according to Eq (A.1) and the values of $F(x_i)$ are computed using expected rank of Eq (A.2). In addition, the true rank of each sample, which is the random number used to compute x_i is used for the purpose as a point for comparison with the expected rank. It must be reiterated that the true rank of any data point will almost never be absolutely known.

1. Simulation Software

```
% MATLAB program to compare nonparametric method of describing a set of
% data using expected rank with the known or underlying distribution of
% the data set
%
% Developed by: LT James W. Coleman, USN
%
```

```
% Prompt user for input of the number of samples in the data set, the
% number of simulated data sets desired, and the underlying parameters
% of the Weibull distribution used to form the data set.
%
n=input('Enter number of samples in the data set ');
iter=input('Enter number of simulations desired ');
alpha1=input('Enter underlying value of shape parameter alpha ');
beta1=input('Enter underlying value of location parameter beta ');
%
% Compute the expected rank for each of the samples, and transform to
% the ln-ln space F* to linearize CDF. Note that expected rank depends
% only on the number of samples in the data set.
%
erank=[1:n]/(n+1);
fstar=log(-log(1-erank));
%
% Perform the simulation as many times as specified.
%
for i=1:iter
%
% Generate a set of random numbers and assign them as the probability of
% failure F(xi). Order the probabilities F(xi) and transform into the
% F* space
%
fxi=rand(1:n);
fxi=sort(fxi);
fstarx=log(-log(1-fxi));
%
% Solve for the values of xi (the set of data) which correspond
% to those F(xi)'s, given the shape parameter alpha and location
% parameter beta. The values of alpha and beta used are the underlying
% parameters and the Weibull distribution used is the underlying distribution.
%
xi=beta1*(-log(1-fxi)).^(1/alpha1);
%
% Compute the expected rank for each of the samples, and transform to
% the ln-ln space F* to linearize CDF
%
erank=[1:n]/(n+1);
fstar=log(-log(1-erank));
%
% Plot the results of the expected rank F and the true rank values F(xi)
% versus the log(xi) in the transformed F* space
```

```
semilogx(xi,fstarx,'-w',xi,fstar,'ow')
pause
%
%  If the simulated data set displays interesting characteristics, the user
%  may save it for later analysis.  File name will have the form xi#.dat.
qsave=input('Enter 1 to save this data set xi, 0 to continue');
if qsave==1
   eval(['save xi',num2str(iter),'.dat xi /ascii'])
   acknw=input('Record parameters used for xi and hit Enter');
end
end
```

B. SIMULATION TO DETERMINE THE DISTRIBUTIONS OF ESTIMATORS

1. Simulation Description

In this simulation, a random set of data is generated using the procedure described above, and the maximum likelihood estimators are computed from the random data set. The algorithm used to determine the MLE's incorporates the Golden Section Method to find the zero of a function of one variable. The equation of α is given as

$$\alpha = \left[\frac{\sum_{i=1}^{n} x_i^{\alpha} \ln x_i}{\sum_{i=1}^{n} x_i^{\alpha}} - \frac{1}{n} \sum_{i=1}^{n} \ln x_i \right]^{-1} \qquad \text{(D.2)}$$

The golden section method is used to find the zero of Eq D.2; the result being the MLE $\hat{\alpha}$. Although not considered an efficient means of determining the zero of a function, the golden section method has the advantage of guaranteed convergence within a computable band of certainty. The MLE $\hat{\beta}$ is determined from the value of $\hat{\alpha}$ by the following equation

$$\beta = \left[\frac{1}{n} \sum_{i=1}^{n} x_i^{\alpha} \right]^{\frac{1}{\alpha}} \tag{D.3}$$

Once the MLE's are computed, they are stored in column vectors. The process of generating the random data set is repeated 10,000 times in order to produce a large number of estimators to be analyzed. The estimators are then sorted using a separate routine so that the results can be viewed in the form of a joint histogram. The marginal distributions are obtained from the joint histogram by applying Eq 3.7. The amount of uncertainty in the estimators can then be determined from the resulting distribution.

2. Simulation Software

```
% MATLAB program which computes the Maximum Likelihood Estimators (MLE)
% of a simulated random data set xi of n samples. The process is repeated
% 10000 times in order to obtain a distribution of the MLE's corresponding
% sets of data of n samples. Each simulated data set has known values of the
% parameters in the Weibull distribution used to construct the data from
% random numbers.
%
% Developed by: LT James W. Coleman, USN
```

```
%
%  Description of the variables:
%  max - Maximum number of repetitions, or # of MLE's computed
%  count - count number of repetitions
%  n - # of samples in the simulated data sets
%  stora,storb - column vectors which MLE's alpha' and beta' are stored
%  alpha1,beta1 - underlying values of the parameters
%  fxi - Probability of failure CDF
%  xi - Simulated random data set with an underlying distribution
%  xl,xu - Upper and lower bounds used when computing MLE alpha'
%  fl,fu - Residual from MLE equation for alpha to be minimized
%  niter - Number of iterations needed to bracket the MLE alpha'
%  x1,x2 - Intermediate values used to compute MLE alpha'
%  f1,f2 - Residuals based on the intermediate values
%  t - Golden Section Ratio
%  k - iterations performed within the golden section method
%  fmin - Minimum residual computed in the golden section method
%  alphah - MLE alpha'
%  betah - MLE beta'
%
%  Initialize variables
%
max=10000;
count=1;
n=10;
stora=zeros(max,1);
storb=zeros(max,1);
%
%  Prompt user for input of number of samples and underlying parameters.
%
n=input('Enter number of samples in the data set ');
beta1=input('Enter underlying location parameter beta ');
alpha1=input('Enter underlying shape parameter alpha ');
%
%  Begin repitition of the simulation
%
while count<=max
%
%  Generate a random data set xi from random numbers assigned as the
%  CDF values F(xi)
%
  fxi=rand(1:n);
  xi=beta1*(-log(1-fxi)).^(1/alpha1);
```

```
%
% Solve for the MLE's using the Golden Section Method to minimize a
% function of one variable. The function solva(alpha,xi) computes a residual
% value f resulting from substituting the guessed value of alpha and the
% data set xi into the equation of ML for alpha. The residual, therefore, is
% the difference between the computed value and the most likely alpha. This
% is the value being minimized.
% Compute residual for the upper and lower bounds xl and xu. These values
% are set at a factor of 10 above and below the underlying values.
%
 xl=alpha1/10;
 xu=alpha1*10;
 fl=solva(xl,xi);
 fu=solva(xu,xi);
% Seventeen iterations are required for interval of uncertainty of 0.00119
 niter=17;
% Determine the lower intermediate value x1 of alpha based on a weighting by
% the golden section ratio t applied to the lower bound. Compute residual
% with this value.
 t=0.381966;
 x1=(1-t)*xl+t*xu;
 f1=solva(x1,xi);
% Determine the upper intermediate value of alpha based on a weighting by
% the golden section ratio t applied to the upper bound. Compute residual
% for this value.
 x2=t*xl+(1-t)*xu;
 f2=solva(x2,xi);
 k=4;
 while k<niter
    if f1>f2
% The residual from x1 is larger than residual from x2; make the old x1
% the new lower bound, x1 (lower intermediate value) becomes the old x2,
% the new value of x2 is computed using the golden section ratio on the
% new bounds. Compute residual for new x2
       xl=x1;
       fl=f1;
       x1=x2;
       f1=f2;
       x2=t*xl+(1-t)*xu;
       f2=solva(x2,xi);
       k=k+1;
    else
% The residual from x2 is larger than residual from x1; make the old x2
```

```
% the new upper bound, x2 (upper intermediate value) becomes the old x1,
% the new value of x1 is computed using the golden section ratio on the
% new bounds. Compute residual for new x1
        xu=x2;
        fu=f2;
        x2=x1;
        f2=f1;
        x1=(1-t)*xl+t*xu;
        f1=solva(x1,xi);
        k=k+1;
     end
  end
% Determine which of the residuals is the lowest and the value of alpha which
% corresponds to that residual.
  fmin=min([fl,f1,f2.fu]);
  if fl==fmin, alphah=xl;, end;
  if f1==fmin, alphah=x1;, end;
  if f2==fmin, alphah=x2;, end;
  if fu==fmin, alphah=xu;, end;
%
% Compute the MLE beta from using the MLE alpha and store both estimators in
% column vectors stora and storb
%
  betah=(sum(xi.^alphah)/n)^(1/alphah);
  stora(count,1)=alphah;
  storb(count,1)=betah;
%
  count=count+1;
  end
% Save the results for later analysis
  save a_510.dat stora /ascii
  save b_510.dat storb /ascii
```

C. SIMULATION TO COMPUTE INFORMATION IN AN EXPERIMENT

1. Simulation Description

The simulation developed here will compute the information resulting in either a schedule censored or number of data censored experiment. The data set generated in the simulation is the expected values of the realized random variable x, which correspond to the expected rank and the underlying values of the parameters specified by the user. The user inputs the the underlying value of α, the number of samples in the experiment, and a vector containing either the scheduled censor locations (fraction of mean) or the censor points based on the fractional number of realized data. The program computes the likelihood of the parameters for each censored data set. The parameter space is defined from 0.25 to 4 times the underlying value of alpha, and 0.05 to 150 times the underlying value of beta. The large range of beta is required when the underlying alpha is less than unity and only a small number of points are realized.

The marginal distributions of the parameters are obtained by projecting the likelihood surface on the respective axes. The marginal distribution of alpha is then integrated and normalized by the resulting area. The information is computed based on the marginal distribution of alpha and stored corresponding to that particular censor location. The process is

repeated until the information has been calculated for each of the input censor points.

2. Simulation Software

```
% MATLAB Program to compute information based on time censored data. The user
% definesthe input %values for the underlying alpha. The location parameter beta is %
fixed at 100 for this particular grid. The vector tcensor defines when the data is %
censored (fraction of the mean). The numerical values of information are
% contained in the vector I.
%
% Developed by: LT James W. Coleman, USN
%
% Define underlying parameters and range of alphas
%
alpha1=input('enter underlying value of alpha ')
alphamax=4*alpha1;
alphamin=alpha1/4;
astep=(alphamax-alphamin)/50;
alpha=alphamin:astep:alphamax-astep;
beta1=100;
%
% User defines number of samples in data set
%
n=input('enter number of samples in the data set ')
%
% Determine the set of expected data, based on expected rank
%
for k=1:n,fxi(k)=k/(n+1);,end
xi=beta1*(-log(1-fxi)).^(1/alpha1);
xi=sort(xi);
qcensr=input('enter 0 for scheduled censor, 1 for censor based on failures ')
if qcensr==0
%
% Define the censor locations as a fraction of the mean
%
  tcensor=input('enter censor points as fraction of mean life ')
  lmax=length(tcensor);
else
  xcb=input('enter censor points as fractional realizations ')
  lmax=length(xcb);
```

```
end
%
%  Initialize variables and the likelihood
%
count=1;
inc=1;
flag1=0;
flag2=0;
L=zeros(50,50);
while count<=lmax
 if qcensr==0
%
%  Determine the time of censor and use this value to define which points are exact
%
    xc=tcensor(count)*beta1
    index=max(find(xi<=xc));
    xie=xi(1:index);
    c=length(xie)
 else
%
%  Determine the exact data and the number of exact data
%
    nreal=xcb(count)*(n);
    xie=xi(1:nreal);
    c=length(xie)
    if c<=1
      xc=xie;
    else
      xc=max(xie);
    end
  end
  beta=5:5:250;
  iter=1;
  while iter<=3
%
%  Compute likelihood (50x50 array) for censored data
%
    L=zeros(50);
    if c~=0
      for i=1:50
       for j=1:50
          a=alpha(i);
          b=beta(j);
```

```
      xib=xie/b;
      L1=((a/b)^c)*prod((xib.^(a-1)).*exp(-(xib.^a)));
      L2=(exp(-(xc/b).^a))^(n-c);
      L(i,j)=L1*L2;
    end
   end
   m=length(alpha);
   a=1;
   b=1;
%
% Obtain marginal distributions of alpha by summing along the betas
%
   for u=1:50,ma(u)=sum(L(u,:));,end
   if iter==1,ma1=ma';,end
   if iter==2,ma2=ma';,end
   if iter==3,ma3=ma';,end
%
% Normalize alphas for a common integration range by dividing astep by
% alpha1
%
   delta=astep/alpha1
%
% Compute the area under the marginal distribution and normalize the values
%
   area(iter)=numintg(m,a,b,delta,ma)
   ma=ma/area(iter);

%
% Compute the information based on the marginal distribution of alpha
%
   info=zeros(50,1);
   if iter==1
    for u=1:50
      if ma(u)~=0.0
        info(u)=info(u)+ma(u)*log(ma(u));
      end
    end
    I(count)=sum(info);
   end
% This test is to determine if the likelihood is required to be computed for the higher
%  values  of beta, such as used in iter=2 and 3.  As more data is realized, the
%  likelihood surface narrows to the region where beta= 5:250; no longer requiring
% the computation for high values of beta.  The test compares the differences in the
```

```
% area from iter=2 to iter=1.  If the area computed in iter=2 is very small compared %
to iter=1, then additional computation of likelihood in that range of betas.
%
     if (iter==2)&(flag1==0)
      diffa12=area(2)/area(1);
      if diffa12<1.e-6,flag1=1,end
     end
     if iter==3
      if flag2==0
        diffa13=area(3)/area(1);
        if diffa13<1.e-6,flag2=1,end
      end
%
%  If all three iterations are required to define the likelihood, revise the previous value
%   of I
%
      info=zeros(50,1);
      mat=ma1+ma2+ma3;
      ma=mat';
%
%  Compute the area under the marginal distribution and normalize the values
%
           areat=numintg(m,a,b,delta,ma);
      ma=ma/areat;
%
%   Compute the information for this censor location
%
      for u=1:50
        if ma(u)~=0.0
          info(u)=info(u)+ma(u)*log(ma(u));
        end
      end
      I(count)=sum(info);
     end
     I
   else
%
%  If no data was realized, set I = 0
%
     I(count)=0;
     I
   end
%
```

```
% Check the flags to determine if large values of beta are required for the next
%  likelihood calcuation
%
   if flag2==1,iter=3;,end
   if (flag1==1)&(iter==2),iter=3;,end
   iter=iter+1
%
% Define the regions for the large values of beta
%
   if iter==2,beta=250:100:5150;,end
   if iter==3,beta=5150:200:14950;,end
%
% Initialize variables for next iteration
%
   ma=zeros(1,50);
   mat=zeros(50,1);
   L=zeros(50,50);
 end
%
% Initialize variables for next iteration
%
 count=count+1
 inc=inc+1;
 L=zeros(50,50);
end
```

LIST OF REFERENCES

1. Shigley, J.E. and Mischke, C. R., *Mechanical Engineering Design*,McGraw Hill, New York, 1989.

2. Rosen, B. W., "Tensile Failure of Fibrous Composites," *Journal American Institute of Aeronautics and Astronautics*, Vol. 2, No. 11, pp 1985-1991, Nov. 1964.

3. Harlow, D. G. and Pheonix, S. L., "The Chain-of-Bundles Probability Model for the Strength of Fibrous Materials I: Analysis and Conjecture," *J. Composite Materials*, Vol. 12, pp. 195-214, April 1978.

4. Harlow, D. G. and Pheonix, S. L., "The Chain-of-Bundles Probability Model for the Strength of Fibrous Materials II: A Numerical Study of Convergence," *J. Composite Materials*, Vol. 12, pp. 314-334, July 1978.

5. Coleman, B. D., "Statistics and Time Dependence of Mechanical Breakdown in Fibers," *J. Applied Physics*, Vol. 29, No. 6, pp. 968-983, June 1958.

6. Phoenix S. L. and Wu E. M., *Statistics for the Time-Dependent Failure of Kevlar-49/Epoxy Composites: Micromechanical Modeling and Data Interpretation*, Lawrence Livermore National Laboratory, Livermore, CA, UCRL-53365.

7. Shannon, C. E., "A Mathematical Theory of Communication," *Bell System Technical Journal*, Vol. 27, No. 3, July 1948.

8. Lindley, D. V., "On a Measure of the Information Provided by an Experiment," *Annals of Mathematical Statistics*, Vol. 27, No. 4, pp. 986-1005, December 1956.

9. Bury, K. V., *Statistical Models in Applied Science*, John Wiley and Sons, 1975.

INITIAL DISTRIBUTION LIST

	No. Copies
1. Defense Technical Information Center Cameron Station Alexandria, Va 22304-6145	2
2. Library, Code 0142 Naval Postgraduate School Monterey, CA 93943-5002	2
3. Chairman, Code 69 Department of Mechanical Engineering Naval Postgraduate School Monterey, CA 93943-5000	2
4. Dr. Edward M. Wu Professor of Aeronautics, Code AA/Wu Naval Postgraduate School Monterey, CA 93943-5000	4
5. Superintendent Naval Engineering Cirricular Office, Code 34 Naval Postgraduate School Monterey, CA 93943-5000	1
6. Dr. Robert Badaliance Naval Research Laboratory, Code 6380 Branch Head/Mechanics of Materials Washington, DC 20375	1

7. Dr. S. C. Chou 1
Chief, Materials Dynamics Branch
Army Materials Technology Laboratory
Attn: SLCMT-MRD
Watertown, MA 02171-0001